NASA CONTRACTOR REPORT

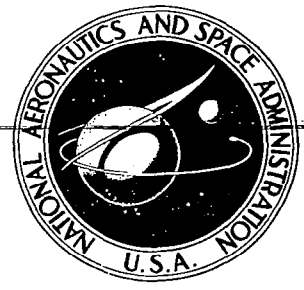

NASA CR-2

NASA CR-2831

METHOD FOR OBTAINING AERODYNAMIC DATA ON HYPERSONIC CONFIGURATIONS WITH SCRAMJET EXHAUST FLOW SIMULATION

William R. Hartill

Prepared by
ROCKWELL INTERNATIONAL
Los Angeles, Calif. 90009
for Langley Research Center

NATIONAL AERONAUTICS AND SPACE ADMINISTRATION • WASHINGTON, D. C. • JUNE 1977

1. Report No.	2. Government Accession No.	3. Rec.
NASA CR-2831		

4. Title and Subtitle	5. Report Date
METHOD FOR OBTAINING AERODYNAMIC DATA ON HYPERSONIC CONFIGURATIONS WITH SCRAMJET EXHAUST FLOW SIMULATION	June 1977
	6. Performing Organization Code

7. Author(s)	8. Performing Organization Report No.
William R. Hartill	NA-76-752
	10. Work Unit No.

9. Performing Organization Name and Address	11. Contract or Grant No.
Los Angeles Aircraft Division Rockwell International International Airport, Los Angeles, CA 90009	NAS1-14320
	13. Type of Report and Period Covered
12. Sponsoring Agency Name and Address	Contractor Report
NASA Langley Research Center	14. Sponsoring Agency Code

15. Supplementary Notes

Final report

Langley Technical Monitor: James M. Cubbage

16. Abstract

This report describes a hypersonic wind tunnel test method for obtaining credible aerodynamic data on a complete hypersonic vehicle (generic X-24c) with scramjet exhaust flow simulation. The general problems of simulating the scramjet exhaust as well as accounting for scramjet inlet flow and vehicle forces are analyzed and candidate test methods are described and compared. The method selected as most useful makes use of a thrust-minus-drag flow-through balance with a completely metric model. Inlet flow is diverted by a fairing. The incremental effect of the fairing is determined in the testing of two reference models. The net thrust of the scramjet module is an input to be determined in large-scale module tests with scramjet combustion. Force accounting is described and examples of force component levels are predicted. Compatibility of the test method with candidate wind tunnel facilities is described and a preliminary model mechanical arrangement drawing is presented. The balance design and performance requirements are described in a detailed specification. Calibration procedures, model instrumentation, and a test plan for the model are outlined.

17. Key Words (Suggested by Author(s))	18. Distribution Statement
Hypersonic vehicle Scramjet Aerodynamic test method	**Unclassified – Unlimited** **Subject Category 02**

19. Security Classif. (of this report)	20. Security Classif. (of this page)	21. No. of Pages	22. Price*
Unclassified	Unclassified	76	$5.00

* For sale by the National Technical Information Service, Springfield Virginia 22161

TABLE OF CONTENTS

LIST OF ILLUSTRATIONS

LIST OF TABLES

METHOD FOR OBTAINING AERODYNAMIC DATA ON HYPERSONIC CONFIGURATIONS WITH SCRAMJET EXHAUST FLOW SIMULATION

William R. Hartill
Rockwell International
Los Angeles Aircraft Division
Los Angeles, California

SUMMARY

This report describes a method for obtaining credible aerodynamic data on a complete vehicle (generic X-24C) with scramjet exhaust flow simulation in hypersonic wind tunnel tests.

Scramjet exhaust flow simulation is provided by injection of a "cold" substitute gas that has been developed to simulate closely the interactions and moments of the scramjet engine (ref. 1). Various methods of arranging and conducting such a test were examined with particular attention given to the ways and means and effects of bypassing the scramjet inlet flow, and accounting for all forces.

The method selected is based on the use of a flow-through, six-component force balance. An inlet fairing bypasses the scramjet module inlet flow. The effect of the fairing and bypassed flow is then determined by force increments measured between reference model configurations designed to isolate the effects.

Analyses were performed to predict the flow fields and forces to be experienced by the models, including those generated by the scramjet simulant gas. These were used to establish design criteria for the force balance and provide baselines for measurement accuracy.

A preliminary model mechanical design was prepared to prove out the practical solution of the test method with particular attention given to plumbing systems, seals, tare forces, balance location, and instrumentation.

A detailed test program has been prepared for test of a 1/30-scale model in the NASA Langley 20-inch Mach 6 wind tunnel. Model requirements, calibration, instrumentation, and test procedure are described for the use of this test method.

INTRODUCTION

The high-speed research airplane (generic X-24C) currently under study by NASA and USAF (figure 1) has, as one of its research objectives, the role of flying test bed for integrated scramjet engines. In preparation for this role, wind tunnel tests are needed to evaluate and predict vehicle aerodynamic performance with the interactive aerodynamic effects of the engines properly simulated.

The scramjet inlet and exhaust flows play a major role in determination of the aerodynamic forces and moments acting on the vehicle, as the entire undersurface is devoted to the propulsion system. It is not feasible to simulate scramjet combustion with an actual scale engine; therefore, other means of simulation have been developed. Scramjet exhaust gas has been simulated with mixtures of Freon and argon by NASA (ref. 1). These substitute gases have been found to have expansion characteristics and behavior close to the hydrogen/air combustion products, but at moderate temperature levels. Injection of these substitute gases into a scramjet wind tunnel model to simulate the exhaust expansion flow field is now feasible.

This report describes a method and plan for obtaining credible aerodynamic data in wind tunnel tests of the high-speed research airplane with scramjet exhaust flow simulation. Preliminary model designs are presented to facilitate expedient construction of models once the mold lines for the configuration are finalized.

SYMBOLS

The moment reference point was located on the fuselage reference line at $x/\ell = 0.65$.

Ar	reference wing area including fuselage intercept, 56.28 meters^2
E	error
F	force
F_3	stream-thrust force, module sta 3 (combustor exit)
F_A	axial force along X axis
F_N	normal force along Z axis
My	pitching moment about Y axis
F_{3A}	stream thrust axial force, module sta 3
F_{3N}	stream thrust normal force, module sta 3
F_3My	stream thrust pitching moment, module sta 3
C_A	axial force coefficient, $F_A/q_\infty Ar$
C_N	normal force coefficient, $F_N/q_\infty Ar$
Cm	pitching moment coefficient, $My/q_\infty Ar\ell$
(a), (b), (c), (d), (e), (f)	model stage (figure 8)
ℓ	vehicle length, 17.53 meters (57.5 ft)
x	axial length from vehicle nose
M_∞	free-stream Mach number
M_3	module sta 3 Mach number

P	pressure
P_∞	free-stream pressure
P_t	total pressure
P_{t^∞}	free-stream total pressure
P_3	module sta 3 pressure
q_∞	free-stream dynamic pressure
R	unit Reynolds number
R_∞	free-stream Reynolds number based on vehicle length
T	temperature
T_t	total temperature
W_3	simulant gas flow rate at sta 3
α	angle of attack
β	fuselage lower surface angle, 3.5 deg
ψ	angle of side slip
ϕ	equivalence ratio

TEST METHOD ANALYSIS

The scramjet exhaust flow does not lend itself to simulation of the direct duplication of the supersonic combustion process for the following reasons:

(1) High stagnation pressures and temperatures are needed in the ground facility to support the scramjet combustion reaction. These conditions are costly, difficult to achieve in a reasonable size, and require model thermal protection.

(2) Large-scale combustors and nozzles are needed to duplicate the complex aerodynamic, thermodynamic, and chemical processes which occur in a scramjet nozzle. The processes are not geometrically scalable primarily because the chemical reactions proceed as functions of stay time.

(3) Hydrogen injector design and the mixing process exert a strong influence on the combustion and expansion process. Scaling the injection system is difficult to achieve in providing the desired simulation.

The dilemma posed by the need for exhaust flow simulation and the nonpracticality of scaling a scramjet combustor for use in a state-of-the art wind tunnel model has led to the technique of injecting a substitute cold gas to simulate the exhaust (ref. 1). Such a scheme appears to be satisfactory from the standpoint of matching the desired pressure distributions over a scale model nozzle; it is now desired to incorporate this scheme in a wind tunnel model.

With this anticipated solution of the nozzle gas flow problem on the model, other questions surface and become predominant. These have to do with the means of getting the simulant gas onboard the model without causing balance tare loads that are large in relation to vehicle model forces, or tare loads that are functions of temperature, hysteresis, pressure, or other variables that are often difficult to calibrate and compensate. Means must also be provided to measure (or otherwise calculate) the thrust and moments created by the simulant gas separate from the forces reacted by the expansion nozzle and airframe.

Since the scramjet exhaust is to be replaced with a substitute gas, means must be provided for eliminating, bypassing, or otherwise disposing of the

inlet airflow. The manner in which this is accomplished is critical for the following reasons:

(1) The inlet-flow field scrubs a relatively large area of the vehicle body, and alteration of this interaction would have significant effects on the vehicle lift, drag, and moments.

(2) The inlet stream-thrust force is large compared to the other vehicle forces, and deficiencies in accounting for this force can lead to error magnification in the summation of vehicle forces.

(3) Fairings, pipes, and other alterations to the simulated vehicle for accommodating the inlet flow can cause unrepresentative tare forces and, also, unrepresentative interactions between forebody flow fields and nozzle flow fields.

The solution to these problems must be involved with realistic, attainable mechanical systems, instrumentation, and test facilities, and the methods must reflect appropriate safety and economic standards.

Test Methods

A survey of candidate test methods potentially suitable for models with scramjet exhaust flow simulation was conducted. Six candidate methods are outlined, with advantages and disadvantages of each discussed.

Method A. -

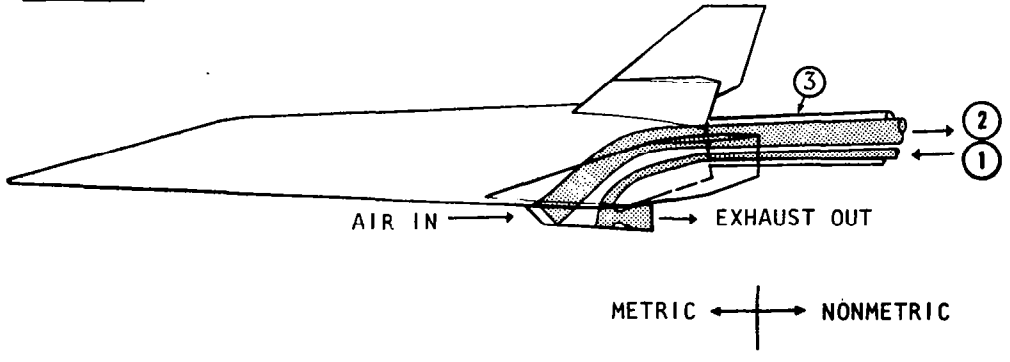

① Simulated scramjet exhaust gas supply

② Inlet flow captured and exhausted outside of tunnel

③ Two gas systems pass through balance

Method A uses the direct approach of ducting the simulant gas into the vehicle model and ducting the inlet air out of the model. All engine flows are simulated simultaneously in one model, with no modifications of the model external lines. Basic model forces are measured on a six-component internal balance.

Entering and exiting momentum of the two gas flows must be measured and accounted for. The primary problem with this approach is the design of the inlet air duct to pass the required flow rate without choking and increasing the inlet spillage.

The sharp turn required at the inlet module would add to the flow losses, and it is doubtful that sufficient flow area could be obtained within the sting/balance cross section without causing large base pressure interactions. Ducting of the two separate gas flows across the balance would add to the complexities of design and calibration procedures.

Method B. -

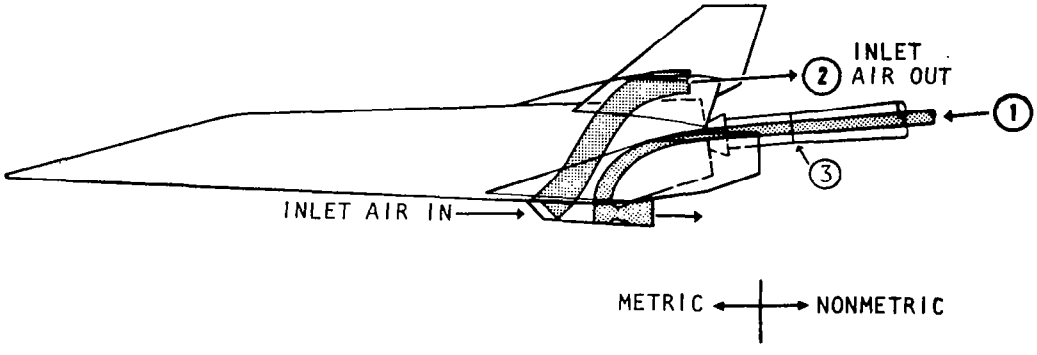

① Simulated scramjet exhaust gas supply

② Inlet flow captured and exhausted on top of model

③ One gas system passes through balance

Method B is a modification of A in which the inlet air flow is ducted to the top of the vehicle model and is exhausted into the free stream. This approach keeps the balance relatively simple, since only the exhaust nozzle simulant gas goes across the balance.

Difficulties with this system are the accounting of the nonvehicle lines and air exhaust forces on the top of the model. Also, as in plan A, the inlet duct may cause nonsimulated inlet spillage. Application of this method in handling the inlet flow in the model of reference 2 did result in an unstarted inlet and unknown spillage effects.

Method C. -

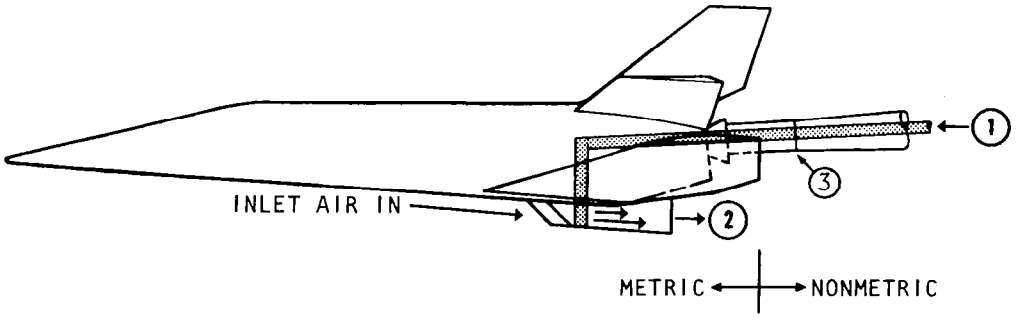

① Special gas supply

② Gas injected and mixed with inlet air to simulate scramjet exhaust flow

③ One gas system passes through balance

Method C is an attempt to simulate closely the scramjet propulsion in a more direct manner. Here the inlet air passes through the scale engine modules, and a simulant gas is injected and mixed to simulate the scramjet exhaust. For this scheme to operate properly, the injected gas would have to be chosen such that the mixture with the inlet air would expand and produce the desired

pressure distribution at the nozzle expansion surface. Development of this gas would require additional work. Advantages of this method are that all flows, inlet and exhaust, are simulated simultaneously and the vehicle lines are uncompromised. Disadvantages include the difficulty in determining proper gas chemistry for injection and the difficulty in getting good mixing between the inlet air and the injected gas.

Method D. -

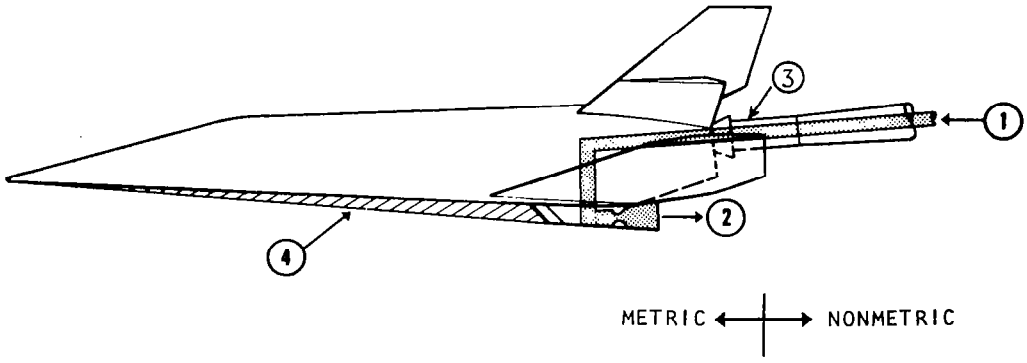

① Simulant gas supply

② Scramjet exhaust simulation

③ Six-component flow-through balance

④ Inlet fairing

Method D uses a faired-over inlet and a series of modified and reference models to determine the effect of the fairing and build up the incremental contributions to the vehicle forces. This method avoids the difficulty of simultaneously simulating inlet and exhaust flow in the same model. The separate effects are isolated in separate tests. Disadvantages are that additional models, test and calibrations are required, and flow interactions between inlet and exhaust are not fully simulated.

Method E also uses a faired-over inlet as shown in ⓐ . Simulant gas is brought onboard and is injected at the model combustor exit. The major parts of the model, including the modules and gas injection system, are nonmetric. This eliminates the need for a static thrust calibration and simplifies the design and calibration of the balance.

Method E. -

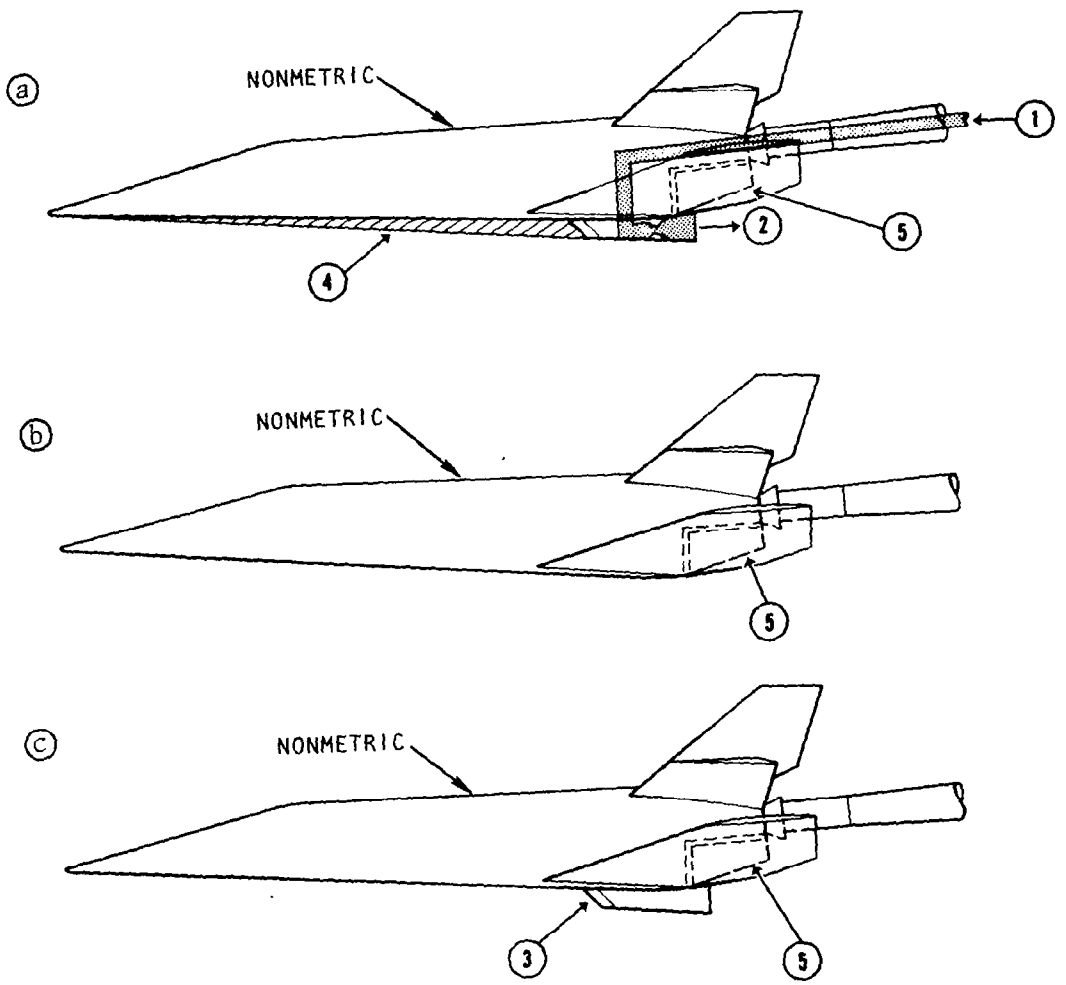

① Simulant gas supply

② Scramjet exhaust simulation

③ Flow-through modules

④ Inlet fairing

⑤ Metric nozzle expansion surface

The area of primary interest, the nozzle/afterbody expansion surface and the immediately surrounding vehicle surfaces, is metric. The exact split-line location would depend on a number of considerations, including cavity pressure stabilization, leakage, and crossflow.

Testing in modes ⓑ and ⓒ provides the means of incrementing the gas expansion effects with the flow-through and clean configuration.

This approach assumes that predictions can be made as to the extent of the propulsion-influenced area of the vehicle, for selection of the split line.

Advantages of method E:

- No gas flows carried across balance.
- No inlet flow to carry across model and/or through balance.
- Experimental accuracy improved, as inlet momentum not measured.
- Momentum of injected gas is nonmetric. Needs no static thrust calibration.

Disadvantages of method E:

- Interaction between inlet spillage and exhaust flow not fully simulated.
- Choice of metric-nonmetric split line critical. Not certain what areas will be influenced by engines.

  Odd-shaped metric-nonmetric split line will be difficult to seal, and cavity pressures difficult to measure.

Method F is a complete static-pressure/area integration of the entire vehicle model. Two basic steps, ⓐ and ⓑ , in model configuration would give the data needed to account for the inlet fairing and the simulant gas injection.

Friction drag is not measured with this method. Analytical estimates of friction drag can be calculated using the turbulent method of Spalding and Chi for the unit Reynolds number and mean wall temperature along the nominal flight path.

Method F.

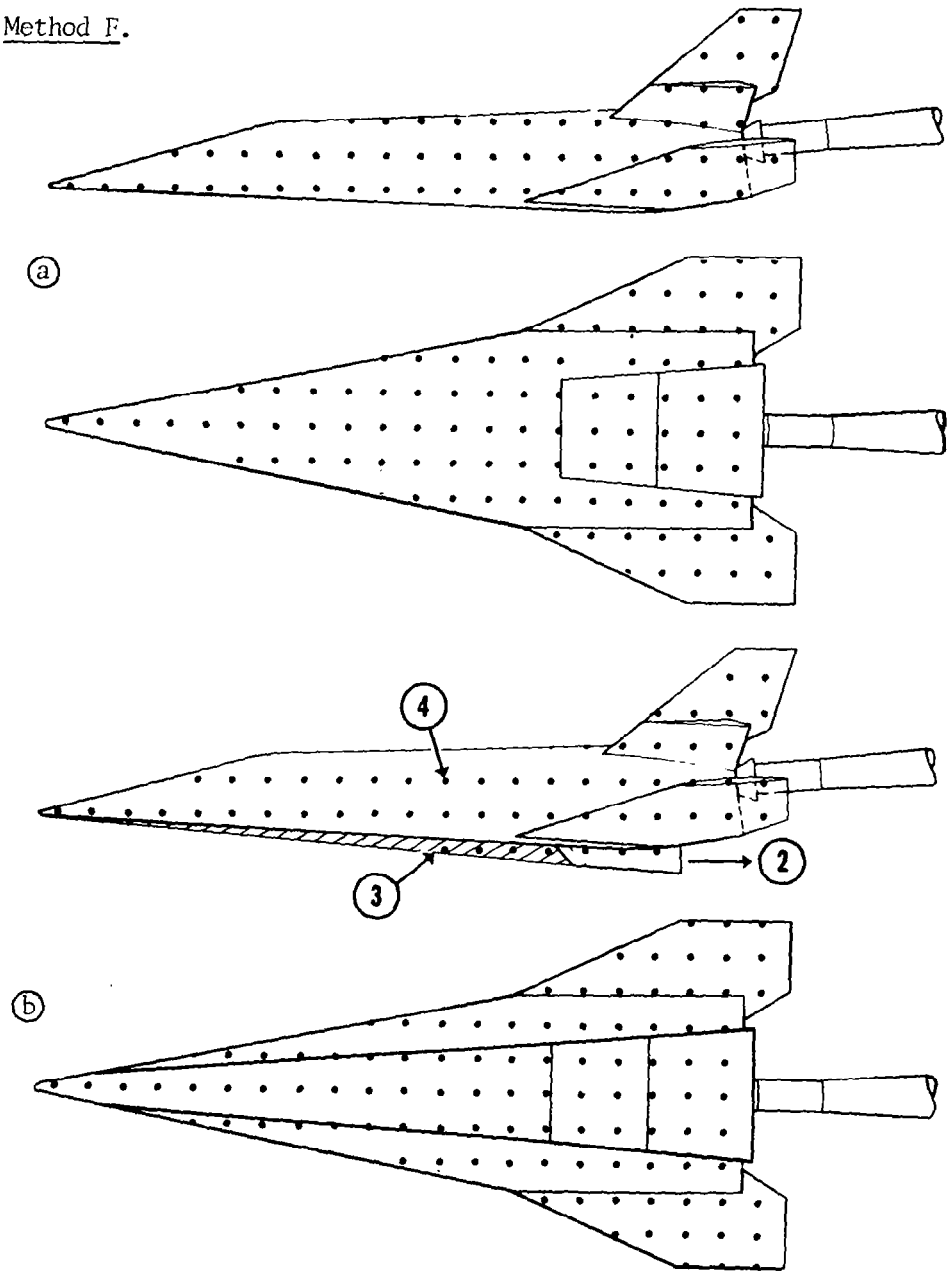

① Simulant gas supply

② Scramjet exhaust flow simulation

③ Inlet fairing

④ Static-pressure orifices

It is estimated that 500 to 800-static-pressure taps would be needed to obtain reasonable accuracy of measurement of the vehicle model forces. This estimate assumes a symmetrical distribution of static-pressure taps over the entire model. Tap spacing would be a function of analytically predicted pressure gradients.

A lesser number of taps, on the order of 300 to 500, could be used if they are placed on one-half of the model so that symmetry of surfaces and measurements are taken into account. This approach would simplify the routing of pressure lines but special care would have to be taken to assure that the model was truly symmetric and that it was aligned correctly in the wind tunnel flow.

In either case, the correct distribution of static taps depends on an accurate prediction of the surface pressure gradients. The ability to make these predictions, particularly in regions of complex three-dimensional flow, is limited.

The advantages of method F:

- No balance calibrations needed (no balance).
- No tare forces due to leakage, flow, or gas injection.
- Diagnostic pressure measurements available.

Disadvantages of method F:

- Large number of static-pressure tubes needed to measure increments, due to inlet fairing and exhaust gas simulation.
- Complex flow fields may be difficult to cover with finite-measurement patterns.

Method G uses a six-component shell balance of the entire model, leaving the simulant gas passage and module internal surfaces nonmetric. A fairing would cover the inlet, and the fairing effect would be determined in separate tests as in methods D and E. All external aerodynamic forces would be measured by the metric part of the model including the nozzle external expansion surface. Advantage of this system is that internal gas flow would not be taken across balance elements, avoiding some of the balance calibration complications that may be encountered with method D. Disadvantages are the difficulty in isolating the nonmetric module exhaust nozzle from the metric module. In this type of model, increased base areas would be needed at the trailing edges of the module exit to fit in the metric/nonmetric gaps. These difficult-to-design base regions are in a sensitive area of steep pressure gradients.

Method C. -

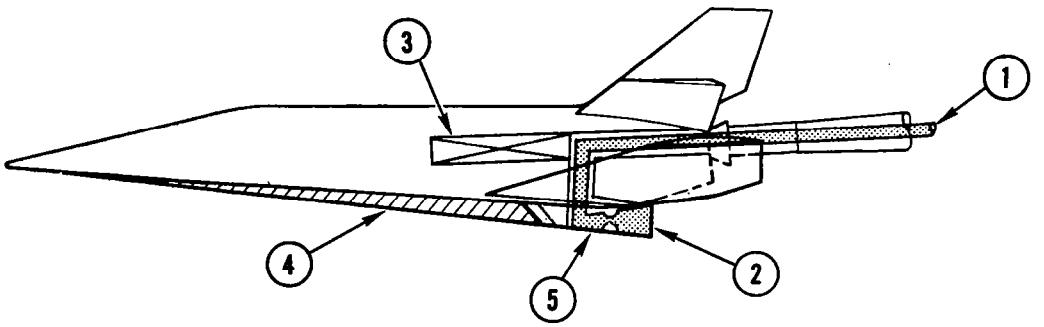

① Simulant gas supply
② Scramjet exhaust simulation
③ Six-component shell balance
④ Inlet fairing
⑤ Nonmetric gas passage

Method Selection

Methods A and B both assume that the inlet capture flow and the injected exhaust simulant gas can be accommodated within the scramjet module geometry simultaneously. This is not feasible, without accepting greater inlet flow spillage, and/or substantially increasing the length of the modules. Either of these solutions would introduce deviations of the scaled vehicle force characteristics. The volume required in the scramjet modules for accommodating the plenum, flow conditioning plates, and expansion nozzle for the injection of simulant gas is about equal to the entire module volume. To additionally require that the inlet flow be captured and turned into the fuselage using the available module space is not practical. Maximum turning geometry permissible would be determined by the detachment limit of the initial angle, rate of turn without flow separation, and duct shape to avoid shock coalescence, and shock-induced boundary layer separation. It is estimated that a redesigned inlet for turning the flow up into the fuselage without altering the desired spillage characteristc would require a length equal to one module length. It is clear that these conflicting design requirements are incompatible.

The ejector mixing scheme of method C is not practical because considerably more work would be required to develop suitable ejector gas constituents and injector designs. It is doubtful that such a gas could be found. The current effort is not geared to this approach.

The method D appears to be sound, and no major problems have been uncovered to reject its consideration.

Although method E takes a convenient, direct approach by providing for the measurement of forces on only the nozzle expansion surface, the difficulty comes in attempting to define and isolate that surface. Also a close examination of the local pressure gradients around the scramjet module and nozzle expansion surface indicates that metric breaks in or near these areas would be risky. Models built in this manner in the past have run into trouble with inconsistent results due to fluctuating, difficult-to-measure cavity pressures. Leakage and shocks from surface mismatch would also create improper aerodynamic interactions.

Method F provides a simpler, less expensive test technique through the use of pressure/area integrations but with some reduction in precision expected. A survey of pressure/area integration derived force data compared with force-balance data from the same wind tunnel models, indicated a preference for the force-balance data, as regards precision. A large number of pressure orifices are needed to cover regions of high-pressure gradients and it is difficult to predict with accuracy where these gradients will be located. With large numbers of pressure orifices it is inevitable that some will leak, be slow to respond, or have calibration errors. These pressure instrumentation faults are often more difficult to detect than a balance reading error during a test.

If the simulant gas is brought on board the model and exhausted from the module through a nonmetric duct, as in method G, the remainder of the model can be metric. This is the "shell balance" method. The balance can be isolated from the simulant gas avoiding some of the temperature sensitivity problems of the flow-through balance. On the other hand, the shell balance requires that a metric/nonmetric split line be provided between the nozzle and the rest of the model. Since the nozzle expansion surface forces are of prime interest in the proposed test, it would be difficult to locate the split line in an area that would not exclude surfaces of interest or create flow disturbances. In addition, the split line must be bridged by a flexible diaphragm to limit the metric surface area that is affected by a tare pressure force. If this is not done the tare force becomes large in relation to the force of interest, and the pressure/area integral on a large irregular surface must be determined. It may be difficult to provide a diaphragm across an irregular shaped split line, and in any event the pressure loading on the diaphragm creates a tare force that must be measured and accounted for.

The seven candidate methods were rated for display in a matrix which compares their effectiveness in meeting the program requirements. A rating of 10 was given to the "best" method/requirement match over the 0-to-10 range, although this rating system is admittedly subjective in nature, it does help in comparing the method features.

METHOD SELECTION MATRIX

Requirement	Method						
	A	B	C	D	E	F	G
Inlet Flow Simulation	4	4	10	8	8	9	8
Exhaust Flow Simulation	10	10	5	10	10	10	10
Exahust Flow Force Measurement	10	10	8	10	6	7	8
Nozzle Geometry Simulation	10	10	10	10	8	10	6
Calibration Precision	7	8	7	8	9	10	9
Force Bookkeeping Precision	8	6	6	9	10	7	9
Total Score	49	48	46	55	51	53	50

The method D emerges from the matrix with best score and it is this method which also appears to be most suitable from the state-of-the-art experience judgement factors exercised in this study.

Methods A, B, and C appear to be out of the running. Methods E, F, and G have potential but are considered to be technically handicapped in various small degrees. Method F for example, although not as highly rated as D, would be a superior choice if more emphasis were given to low-model cost.

The choice of method D is based on maximizing the opportunity to obtain credible aerodynamic data.

Force Analysis

The following definitions are stated here to clarify the distinction between vehicle forces and propulsion forces (figure 2).

(1) Vehicle Forces - Aerodynamic forces generated by the entire vehicle surface not subtended by the propulsion system components (inlet, exterior cowling, and nozzle). This includes the vehicle forebody ahead of the inlet entrance and the base region around the rocket nozzle, but it does not include the scramjet nozzle upper wall or lower cowl lip.

(2) Propulsion Forces - Engine module forces are all forces generated internally in the propulsion module defined as that region subtended by the inlet capture entrance through to the combustor exit. It includes the resulting net thrust (module thrust) and net module lift,

pitch, and, yawing moments. Nozzle forces include all forces generated by the upper nozzle wall and the interior cowl wall downstream of station 3, the combustor exit. External propulsion forces include all forces acting on the external surfaces of the modules including forces induced on the adjacent vehicle surfaces by inlet spillage and the pressure field of the modules.

The force analysis and accountability of method D is based on the use of six model stages. All six stages are built up from the same model pieces to assure uniformity. The stages are denoted by subscripts (a) through (f) and are depicted in figure 3.

(1) Stage (a) is the complete X-24C configuration without scramjet module.

(2) Stage (b) is stage (a), but with the aft portion of the fuselage and wings truncated at a plane normal to the vehicle reference plane at the beginning of the nozzle expansion surface. This truncation also removes the vertical fin.

(3) Stage (c) is stage (b) with scramjet modules and inlet fairing added. The modules contain the thrusting nozzles.

(4) Stage (d) is stage (b) with flow-through engine modules added.

(5) Stage (e) is stage (a) with flow-through engine modules added.

(6) Stage (f) is stage (a) with the scramjet modules and inlet fairing. The modules contain the thrusting nozzles.

The X-24C vehicle will be flown in three different modes. It will be necessary to consider the method of obtaining aerodynamic data on each mode to evaluate properly scramjet exhaust flow effects.

The three modes are:

Mode 1. The X-24C vehicle without scramjet modules. This mode is represented by model stage (a). Forces and moments can be measured directly without configuration simulation corrections, except for the conventional balance and base pressure tares.

Mode 2. The X-24C vehicle with scramjet modules attached, but with $\phi = 0$. This mode is represented by model stage (e). The modules are flow-through configurations in which fuel injection and combus-

tion is not simulated. Forces and moments can be measured directly without configuration simulation corrections, except for the conventional balance and base pressure tares.

Mode 3. The X-24C vehicle with scramjet modules attached and with exhaust flow simulated. This mode must be built up and synthesized by combining data from several model configurations.

Force accounting plan for mode 3. - Model stage (f) consists of the complete vehicle representation including blowing scramjet modules to simulate the scramjet exhaust. The module inlets are shielded by a fairing that introduces a variance in the flow field about the model, resulting in extraneous forces that must be accounted for. The effect of the fairing can be determined by testing model configurations (b), (c), and (d). Force increments measured between models (b) and (c) define the effect of fairing and modules. These models are truncated at the module exit in order that the additional effect of the fairing and modules on the nozzle expansion surface (aft fuselage) is not added to the measured balance forces. In obtaining the increment $\Delta F(b)$ (c) between (b) and (c), a correction must be made for the change in base pressure at the truncated section. Static-pressure instrumentation located in the base area can be used to define the base-pressure force. This approach makes the assumption that the secondary effect of the fairing and modules on that portion of the wings that are truncated is not significant.

Force increments measured between models (b) and (d) define the effect of the unfaired flow-through modules without a nozzle expansion surface. In obtaining the increment F(b) (d) between (b) and (d), a correction must be used for the change in base pressure at the truncated section.

The correction of the force data obtained with configuration (f) to simulate flight with scramjet power, then, consists of the following synthesis:

$$F\ (\text{flight}\ \emptyset = 1) = F\ (f) - F\ (c) + F\ (d) - F_3\ (d)$$

Since the stage (b) configuration drops out in summing the force increments it is not necessary to test stage (b).

The term F_3 (d) represents the forces and moments at the simulated combustor exit station (3) of the flow-through modules of stage (d) configuration. These forces and moments must be removed from the force-accounting equation. The station (3) forces and moments of the simulated power-on scramjet are provided by the injected simulant gas and are measured on the balance of the stage (f) model.

The value of F_3 (d) can be determined by two methods:

(1) Analytically determine stream thrust and angle from theoretical calculations using predicted inlet and module efficiencies.

(2) Calculate stream thrust and angle from experimental inlet and module data, as for example ref. 3.

Alternate force accounting plan for mode 3. - An alternate method is available for force accounting which avoids the necessity of defining the forces F_3(d).

However, this method requires as an input, the net module forces generated with scramjet combustion. The force synthesis is as follows:

$$F\ (\text{flight } \emptyset = 1) = F\ (f) - F\ (c) + F\ (b) - F_3\ (c) + F\ (\text{net module})$$

As in the first plan described, the force increment measured between models (c) and (b) defines the effect of inlet fairing and modules. These models are truncated at the module exit in order that the additional effects of inlet fairing and modules on the nozzle expansion surface (aft fuselage) is not added to the measured balance forces. In obtaining the increment ΔF (b) (c) between (b) and (c), a correction must be made for the change in base pressure at the truncated section. Static-pressure instrumentation located in the truncated base region would be used to define the base-pressure force.

The term F_3 (c) represents the forces and moments at the simulated combustor exit station (3) of the blown modules, simulating the power-on scramjet operation. F_3(c) can be measured directly on the force balance in static (no wind tunnel flow) calibrations using model (c). The truncated model (c) should be used for this calibration so that only the forces at the combustor exit are measured without complication of the additional forces of the nozzle expansion surface, or the plume-elevon interaction. The simulated exhaust gas nozzle expansion surface forces and the plume-elevon interactions are included in the forces measured with model stage (f).

The term F (net module) would be an input obtained from scramjet module development tests. These tests are normally conducted with an external flow field that simulates the local flow properties to be found under the vehicle. Thus spillage, external drag, and module thrust can be defined for the module in tests separate from the vehicle.

The main advantage of this alternate force accounting method is that the difficulty in determining F_3 (d) is avoided. It is believed that measurement of F_3 (c) would be more easily done and would be more accurate. The input F (net module) introduces an element of potential error but it should be noted

that the first method is also subject to this same error. This is so because the simulated combustor exit stream thrust in both methods is based on the duplication of forces predicted by scramjet module tests. How well this prediction matches the flight case is the same for both methods.

Inlet fairing and model truncation effects. - The inlet fairing diverts air around the modules and so modifies the true flow-field that would be obtained with a flowing inlet. This modification of the flow-field is kept to a minimum by making the inlet fairing long and matched to the vehicle body shape. Also, analytical techniques can be used to contour the fairing to more nearly simulate the resulting pressure fields on the modules and vehicle.

Use of the inlet fairing is expected to restrict testing to angles of yaw of no more than a few degrees as the fixed, symmetric fairing geometry would significantly alter the crossflow patterns at greater yaw angles.

Additionally, it should be noted that the truncation of models (b), (c), and (d) removes a portion of wing and elevon surfaces whose increment of forces may be influenced by the presence of the inlet fairing and/or modules. The assumption has been made that these effects are not significant. However, the possibility of significant effects should be investigated using a pressure-instrumented model. This would allow the detection of the presence and magnitude of the pressure field interactions with and without truncation. Force accounting corrections, if found to be needed, could make use of the pressure data, or the force model tests could be continued with a portion or all of the truncated wing restored.

The testing of a pressure-instrumented model would be useful for evaluating the inlet fairing and model truncation effects and, also, validation of the force model testing procedures. The pressure data would provide diagnostic information for analysis of the force data. The pressure-instrumented model would be relatively easy to build and testing could be done prior to construction of the more complex force model.

Analytical Techniques

Analytical predictions of vehicle forces and flow fields were made to establish the relative level of forces involved and to check the sensitivity of nozzle forces to variations in external flow field and simulant gas composition.

A three-dimensional (3D) inviscid calculation of the flow field about the X-24C body was carried out using the finite difference analysis of Paul Kutler, NASA ARC (ref. 4) for Mach number 6.0, angle of attack of 3.0 degrees

and a perfect gas with $\gamma = 1.4$. Flow-field properties at the scramjet module calculated from this program were used as inputs to the exhaust flow interaction analysis.

The exhaust flow analysis uses the Rockwell Integrated Scramjet Nozzle/Afterbody Performance Analysis Method (ref. 5). The method uses the shock capture technique with real gas thermodynamic properties for frozen and equilibrium compositions. It computes internal and external flow fields with multiple shock interactions. Interaction of the exhaust (under or over expanded) with the external stream and vehicle afterbody is considered.

Sample calculations in support of this study program were made to show the effect of exhaust gas composition. Cases were 58% Freon 13B1 + 42% argon, 40% Freon 12 + 60% argon, 100% air, and hydrogen + air combustion products.

It was found that the 58% Freon 13B1 mixture gave near identical pressure distribution to the H_2 + air case, with the 40% Freon reasonably close, and with the 100% air a poor match. These results are plotted in figure 4.

Stream thrust and moment calculations can be made using these analytical pressure distributions. An example of the predicted forces computed in this manner is shown in table I. Again, the relative standing of the simulant gases is apparent.

These analytical procedures were used to predict model forces for use in the balance and model design.

MODEL DESIGN

Detailed preliminary model design drawings have been prepared to illustrate the feasibility of the test method and to facilitate construction of the model once the mold lines for the X-24C are finalized. The 1/30-scale basic model drawing is shown in figure 5. Sketches of the model stage definition showing the variations in model assembly for force accountability are depicted in figure 6. A list of the basic external model parts required to assemble the various model stages is given in table II.

The outer mold lines of the vehicle were based on the NASA LRC X24C-L16 Force Model drawing 24C-200. The scramjet module design was based on the NASA LRC drawing "Airframe-Integrated Scramjet" 1A modified as follows.

Number of modules was reduced from six to five. All dimensions of the modules were increased to simulate a 0.559 m (22 inch) deep module, rather than the 0.457 m (18 inch) design.

These module changes were made to provide a better fit on the bottom of the fuselage and also to increase total engine size to increase thrust level.

Model Scale and Candidate Facilities

The model scale of 1/30 was chosen with consideration of the conflicting requirements of simulant gas flow limits, wind tunnel blockage, Reynolds number simulation and balance size.

The first step was to define the flight conditions that are to be simulated by the model test. The X-24C research vehicle is in preliminary design and analysis and only an approximate set of flight conditions can be given at this time. The altitude Mach-number regime is bounded by constant q lines of 47.88 kN/m^2 and 71.82 kN/m^2 from Mach 4 to Mach 10. Primary interest at present is at $q = 47.88\ kN/m^2$ and Mach 4 to 7. Additional capability from Mach 3 to Mach 8 would be useful. This general flight regime is shown in figure 7, which shows that the scramjet experiment will be operating at a unit Reynolds number between $3.28 \times 10^6/m$ and $9.84 \times 10^6/m$.

Next step was to define the scramjet nozzle exit flow Mach number and pressure ratio that is to be simulated. The simulated combustor exit is to be provided in the model such that the correct Mach number (M_3) and exit pressure ratio (P_3/P_∞) are established with the simulant gas. These variables are dependent, to some degree, on the equivalence ratio, combustor efficiency, and inlet efficiency, and also to the vehicle angle of attack. However, these effects are generally small, within the band of optimum conditions desired for the scramjet experiment. The general trend of M_3 versus M_∞ is shown in figure 8.

A study of the scramjet data of reference 6 indicates that nominal values of combustor exit pressure ratio (P_3/P_∞) over the free-stream Mach number range will be as depicted in figure 9. At the lower Mach numbers (below 4), it is expected that $\phi = 1.0$ may not be possible, and it is not yet known what the limits will be on the various modes of combustion. In any event, the ranges shown in figures 8 and 9 were used in the model analysis.

The characteristics of candidate wind tunnels were then examined to determine the most reasonable model scale and to establish a test plan. Five candidates chosen for study are listed in table III. They are described as follows:

Facility 1 - NASA Langley 20-Inch Mach 6 Wind Tunnel. - This facility is a blowdown tunnel which utilizes a contoured 2-D nozzle block to achieve Mach 6. A sting-support-mode mounting system is available. The test section is 0.508 m (20 inches) square with a usable test core of approximately 0.406 m x 0.406 m.

Facility 2 - NASA Langley Unitary Plan Wind Tunnel. - This facility is a closed circuit, continuous flow, variable density tunnel with two legs. Each leg has a 1.22 m x 1.22 m x 2.13 m test section. Leg No. 1 operates from M1.47 to M2.86. Leg No. 2 operates from M2.29 to M4.63. A maximum Reynolds number of 26.6 x 10^6 per meter is available at M4.63.

Facility 3 - NASA Ames 3.5-Foot Hypersonic Wind Tunnel. - This facility is a closed-circuit, blowdown, wind tunnel utilizing interchangeable contoured axisymmetric nozzles. The tunnel can be operated at Mach 5, 7, 10, and 14. The tunnel can accommodate models up to 0.61 m in span, 1.02 m in length and 0.25 m in diameter on straight or bent sting supports. A quick-inserting strut is available to insert models into the test stream that will accommodate models to 0.43 m in span and 0.61 m in length. Insertion time is approximately 1/2-second. Data recording is on magnetic tape, at rates to 2500 samples per second, and reduced off site on an IBM 7094 system. This facility is capable of four runs per day.

Facility 4 - AEDC VKF Wind Tunnel A. - This facility is a 1.02 m by 1.02 m continuous, closed-circuit, variable-density wind tunnel with a range of Mach 1.5 to 6. The model is mounted on a support which is injected into the airstream and translated upstream to the test section.

Facility 5 - AEDC VKF 50-Inch Hypersonic Wind Tunnel B. - This facility is a closed-circuit type with axisymmetric contoured nozzles for Mach 6 and 8. The model mounting system is the same as for Tunnel A.

The simulant gas supply system being constructed for use in the proposed test is located at facility 1, the Langley 20-inch Mach 6.0 tunnel. Although the system is not readily portable, it could be moved to an alternate facility if necessary. The simulant gas system is restricted to a maximum simulant gas mass flow of 0.907 kg/sec at maximum stagnation temperature of 533° K and pressure of 17 atm.

Facilities 1, 4, and 5 were selected for additional study as they appeared to be the most appropriate from the general standpoint of Mach number, and model size.

The maximum Reynolds number based on model length, ($R_{\infty,}$) as a function of model scale was calculated for each of these three candidate facilities, assuming a full-scale characteristic length, ℓ , of 17.53 m. R_∞ was also calculated for each facility with restrictions based on observing maximum simulant gas flow rate, and M_3 and P_3/P_∞, as per the schedule of figures 8 and 9. These model-scale relationships are shown in figures 10 through 15. Also included are the model scale limitations due to test rhombus size and blockage.

In all cases studied it was found that the maximum model size could not be used without exceeding the simulant gas-mass-flow-rate capacity or without reducing the Reynolds number. The optimum model scale for AEDC tunnel A at Mach 6.0 is 0.055, while for the Langley Mach 6.0 tunnel it is 0.035. The higher pressure of the Langley tunnel, however, gives a higher unit Reynolds number. Therefore, in spite of the smaller scale the Langley-sized model would permit testing at $R_\infty = 17 \times 10^6$ (scale = 0.035) compared to $R_\infty = 13 \times 10^6$ (scale = 0.055) for the AEDC tunnel A sized model.

The Mach 4 and 5 operating points of AEDC tunnel A shift the optimum model scale to 0.036 and 0.040, respectively.

The Mach 6 and 8 operating points of AEDC tunnel B shift the optimum model scale to 0.047 and 0.048, respectively.

A model scale of 0.042 would be a good compromise that would permit testing in all candidate facilities at near maximum Reynolds number. A closer examination of testing experience with the Langley Mach 6 tunnel, however, indicated that some difficulty with blockage might be encountered with a 0.042 scale. A blockage model would be required to prove the suitability of that size. With this input, it was decided to base the model design on 0.033 (1/30) scale, the same size as the aerodynamic force models currently being tested by NASA in the Langley Mach 6 tunnel.

Simulant Gas System

The Freon-plus-argon-simulant-gas storage, metering and control system provided by NASA will bring the gas to a connection at the rear of the model support sting. It will be conducted through a minimum 1.9 cm dia-bore-hollow sting to the flow-through balance mounted in the model. At the maximum gas flow rate of 0.907 kg/sec, pressure of 17 atm and temperature of 533° K, the gas flow Mach number will be 0.30, adequate for avoiding choking or large pressure drops.

From the inner bore of the balance the gas is directed through four radial holes to a plenum in the cavity between the balance and model. Both ends of the cavity are sealed with O rings. The bottom of the cavity is open to the scramjet modules, with a metering pressure-drop plate inserted in the opening. The plate and hole pattern can be replaced as determined necessary by flow calibrations.

The simulated scramjet modules and the inlet fairing will be built in a unit to provide adequate room for conducting the gas to the nozzle. A second flow conditioning choke plate will be provided in the modules to help distribute the gas flow evenly to the five nozzle throats. This choke plate will also be replaceable.

The gas is expanded through five vertical throat nozzles to the simulated combustor exit Mach number (M_3). The nozzle blocks will be designed by a 2D method of characteristics and will be replaceable to allow testing at different simulated Mach numbers.

Balance Design

Preliminary model design concepts have been based on experience with a six component flow-through balance used by Rockwell on a number of wind tunnel tests in the B-1 program (figure 16). These concepts led to the writing of a balance design specification which is included in the appendix.

The modified flow-through balance design, as adapted to this test method, is constructed with inner and outer concentric tubes. The outer tube is machined near each end of the balance to form beams that are strain-gaged for force measurement. The inner tube is attached to the outer tube at each end of the balance outside the force-measuring links. A bellows, concentric with both tubes, is placed below the gages to prevent gas leakage through that area. The gas passes from the hollow sting into the inner tube and out through the sides of the outer tube at 90 degrees to the incoming flow direction. The metric model is attached to the outer tube with a plenum to collect the gas and route it through the model to the scramjet modules. The sting is rigidly attached to one end of the inner tube. The opposite end of the inner tube is sealed.

Balance temperature during operation in the Langley Mach 6 wind tunnel will reach an adiabatic level of 541° K or less depending on the run time. High-temperature strain gages will be needed. An example of such a gage, which is commercially available, contains 92% platinum and 8% tungsten. The gage factor is 4.5, stress level is 5.17×10^7 Newtons per meter^2 (7,500 psi) and the operating temperature range is -78° K to +811° K. Automatic modulus compensation on steel is provided.

Proposed technique for calibrating the balance is described in a following section.

TEST PROGRAM

An initial test of the model in the Langley 20-inch Mach 6 wind tunnel is proposed. The scope of the test program should provide a validation of the test method as first priority. Second priority should be to make the measurements needed to define scramjet exhaust gas effects on the basic configuration. Third priority should be evaluation of alternate nozzle and vehicle configurations.

A test period of 160 hours would be appropriate to establish the validity of the method and obtain desired basic data.

Instrumentation

The basic measuring tool for this test is the six-component balance described in the appendix. In addition to the force gages, there will be two thermocouples in the balance, and two static taps and one total-pressure probe in the balance inner-flow tube.

The thermocouples will monitor the fore and aft gage temperature for correlation of gage output sensitivity to heat. The pressures will be used as a check on simulant gas flow rate and internal pressure and gage interactions. Gas flow control and flow rate measurement will be done by the facility gas system to be provided and operated by NASA LRC.

Additional pressure taps will be provided in the model to monitor the gas flow distribution and nozzle expansion surface. There will be three total probes in the module upstream of the nozzle throats. There will be eight static taps distributed on the nozzle afterbody surface. Four static taps mounted on the nonmetric sting will be used to monitor model base pressure. This provides a total of:

2	Thermocouples	Nonmetric side
1	Total pressure probe	
6	Static pressure taps	
3	Total pressure probes	Metric side
8	Static pressure taps	

Calibration

Step 1 of the test plan is to calibrate the flow-through balance.

The strain gage bridges on the balance will first be compensated for zero drift and the change in balance material modulus of elasticity for a temperature change equal to that from ambient to the estimated mean operating temperature.

The balance will then be force calibrated, in an oven, at a temperature equal to the estimated mean operating temperature. Basic slopes will be determined (for all six components) as well as first order, and if required, second order interactions.

Since, during testing, initial and/or final zeros may not be recorded at ambient conditions, the balance will be temperature calibrated while in the oven. Corrections in the form of delta force vs delta temperature will be determined for all components and applied to the zeros recorded during testing. These corrections will also be applied to the data recorded during testing to account for the incremental variations in balance temperature due to variations in simulator gas temperature. (The balance has a thermocouple at each strain gage bridge location.)

The balance will be check calibrated, with weights, at various temperatures in the expected operating range to verify the zero drift corrections and if necessary, determine a calibration slope correction due to change in the balance material modulus of elasticity.

Following the force calibrations, the effect of the simulant gas pressure and weight flow on the balance outputs will be calibrated.

Zero-thrust tares will be measured with flowing gas by attaching a calibration zero-thrust nozzle in place of the scramjet module. The zero-thrust nozzle consists of a large manifold and stilling chamber. Two convergent nozzles exhaust the gas in opposite directions and normal to the model vertical plane. Even though the balance has been designed to minimize forces caused by the flowing gas, experience has shown that a zero-thrust nozzle calibration will show a tare force of 1% or so. The opposite facing nozzles and manifold will be constructed so that they can be reversed, right/left, to balance out possible errors due to manufacturing tolerances.

Upon completion and validation of the balance calibration data, the model will be shipped to NASA LRC and installed in the Langley 20-inch Mach 6 wind tunnel. A thrust calibration of the scramjet module nozzles will be made with the model mounted in the tunnel. For this, the tunnel test section will be evacuated to a very low pressure by connecting it to the exhaust sphere. The simulant gas system connected to the model will be activated and the forces due to the module thrust will be measured on the balance. Model stage configuration (c) will be used for the thrust calibration to avoid extraneous forces on the afterbody expansion surface and to minimize induced flow effects in the test section.

The purpose of the static thrust calibration is to provide data for analysis of component module and vehicle forces.

Test Plan

Upon completion and validation of the thrust calibration data, the configuration testing will begin. The angle-of-attack range will be -5 degrees to +10 degrees. Angle of yaw will be varied from -5 degrees to +5 degrees.

The basic test plan is outlined in table IV. For purposes of counting data points, it has been assumed that there will be four angles of attack and three of yaw. Run 5 is the static zero-thrust calibration run. It would be desirable to make this run prior to the main testing so that the balance calibration can be validated and the results installed in the on-line data computing program.

With gas flow on, a minimum of three nozzle pressure ratios would be desirable to establish parametric relationships. This will not be a continuing requirement after the characteristics of the system are established.

Predicted Forces

Calculations were made using the techniques described to predict the model forces of the selected method D. Axial force, FA, normal force, FN and pitching moment, My, were calculated for a 1/30-scale model test at M = 6, dynamic pressure q = 55 kN/m^2 and $\alpha + \beta = 4$ degrees (Langley 20-inch Mach 6 tunnel).

The results of these calculations are listed in table V. The synthesized representation of forces simulating flight with scramjet operation were derived from the following equations.

$$F_A \text{ (flight } \emptyset = 1.0) = F_A(f) - F_A(c) + F_A(d) - F_{3A}(d)$$

$$F_N \text{ (flight } \emptyset = 1.0) = F_N(f) - F_N(c) + F_N(d) - F_{3N}(d)$$

$$My \text{ (flight } \emptyset = 1.0) = My(f) - My(c) + My(d) - F_3My(d)$$

The normal rated loads of the balance elements are also listed together with the measurement tolerances defined in the balance specification. Refer to the appendix.) A comparison of the predicted loads and balance tolerances gives some indication of system accuracy. However, a meaningful analysis of overall system accuracy must await collection of actual balance calibration data.

A complete error analysis of the proposed testing methods would entail the collection of precision and bias data on all measurements contributing to the test system. This includes many items such as M, Pt, T, W_3, α, ψ, as well as the basic calibration data of the balance.

Such an analysis of the total system accuracy of this test method is beyond the scope of this study as a number of the elements involved are not well defined or measured at this time.

Nevertheless, it is instructive to make a simplified estimate of the expected error, to see if the test method chosen results in an unacceptable error buildup. A buildup in error might be expected because of the dependence on the summation, positively and negatively, of relatively large forces.

The primary source of error in the proposed test method D is the balance. If we use the balance accuracy limits stated in the balance specification (refer to the appendix) as the total uncertainty in each independent model configuration test, an approximate overall error limit can be estimated using the root-sum-square method. The actual error may be more or less depending on the influence of other test measurements and also depending on the actual balance accuracy and repeatability. Nevertheless, this approach is useful to see how the error is influenced by the method.

The balance specification requires that the balance loadings shall produce data which does not deviate more than 0.2% of the normal rated load from the best straight line fit through the data points. This produces the following measurement uncertainties:

Balance Component	Normal Rated Load	Error	Units
Axial	± 31.75 (± 70)	± 0.164 (± 0.14)	Kg (lb)
Normal	± 54.40 (± 120)	± 0.190 (± 0.24)	Kg (lb)
Pitch	± 16.95 (± 150)	± 0.034 (± 0.30)	Nm (in.-lb)

Applying these measurement uncertainties to the force synthesis of method D, and using the alternate force accounting plan for mode 3 and the root-sum-square error summation technique, we have the following analysis:

The increment in force on the afterbody is defined by the force synthesis as:

$$\Delta F \text{ (afterbody)} = F(f) - F(a) - F(c) + F(b) - F_3(c)$$

The estimated error in this force is then:

$$\Delta FE \text{ (afterbody)} = \left[(\Delta FE(f))^2 + (\Delta FE(a))^2 + (\Delta FE(c))^2 + (\Delta FE(b))^2 + (\Delta FE_3(c))^2\right]^{1/2}$$

The resulting estimated errors in the afterbody force components are then listed as follows:

Force Component	ΔF (afterbody)	ΔFE (afterbody)	$\Delta FE/\Delta F$	Error Coefficient
Axial Force	(11.97) lb	(0.31) lb	0.026	$\Delta C_A E = 0.00040$
Normal Force	(14.75) lb	(0.54) lb	0.037	$\Delta C_N E = 0.00070$
Pitching Moment	(-12.85) lb	(0.67) in.-lb	0.052	$\Delta C_m E = 0.00045$

CONCLUSIONS

This study of test methods for obtaining aerodynamic data on hypersonic configurations with scramjet exhaust flow simulation finds the following:

(1) Simultaneous ingestion of inlet flow and ejection of exhaust flow through the scramjet module cannot be accommodated in the available model space.

(2) Shell balance techniques introduce tare forces and surface irregularities that diminish data accuracy.

(3) Pressure area integration offers a lower cost approach but with accuracy limited by difficulty in detecting severe pressure gradients on complex surfaces.

(4) Flow-through balance technique provides best simulation and force accounting.

(5) The test methods require that corrections be made in model module force to account properly for the difference in inlet stream thrust and combustor exit stream thrust. This relationship cannot be simulated directly in a model.

(6) Analytical techniques, in support of the experimental methods, are available for preliminary analysis of forces on the vehicle, including the scramjet exhaust expansion.

(7) Feasibility of a flow-through balance model to 1/30-scale has been indicated by development of a preliminary mechanical design.

(8) Test feasibility and plans have been established to show compatibility with the test method. NASA Langley 20-inch Mach 6 wind tunnel is the optimum facility for initial test.

RECOMMENDATIONS

(1) A wind tunnel test program should be implemented to investigate scramjet exhaust flow aerodynamic effects on a generic X-24C configuration.

(2) The flow-through balance test method described in this study as "Method D" should be used for the program.

(3) An initial test period of 160 hours in the NASA Langley 20-inch Mach 6 wind tunnel should be conducted with the model following the test plan outlined in this study.

(4) The test program should be supported with an analytical study of vehicle and scramjet aerodynamic flowfields and forces.

(5) Consideration should be given to including in the test program a pressure area integration model to explore in more detail the adaptability and accuracy of this less expensive technique.

REFERENCES

1. Oman, R. A.; Foreman, K. M.; Leng, J.; and Hopkins, M. B.; Simulation of Hypersonic Scramjet Exhaust, NASA CR-2494, March 1975.

2. Cubbage, J. M.; and Kirkham, F. S.; Investigation of Engine-Exhaust-Airframe Interference on a Cruise Vehicle at Mach 6, NASA TN D-6060, January 1971.

3. Trexler, C. A.; and Soudera, S. W.; Design and Performance at a Local Mach Number of 6 of an Inlet for an Integrated Scramjet Concept, NASA TN D-7944, August 1975.

4. Kutler, P.; Reinhardt, W. A.; and Warming, R. F.; Numerical Computation of Multi-Shocked Three-Dimensional Supersonic Flow Fields with Real Gas Effects, AIAA Journal, Vol 11, No. 5, pp 657-664, May 1973.

5. Sadunas, J. A.; Integrated Scramjet Nozzle/Afterbody Performance Analysis, AIAA/SAE 11th Propulsion Conference, Anaheim, Calif. 29 September 1975, AIAA Paper 75-1297, 1975.

6. Small, W. J.; Weidner, J. P.; and Johnston, P. J.; Scramjet Nozzle Design and Analysis as Applied to a Highly Integrated Hypersonic Research Airplane, NASA TMX-71972, November 1974.

TABLE I. - CALCULATED SCRAMJET FLOW FORCES AND MOMENTS
HYDROGEN/AIR COMPARED WITH SIMULANT GASES

$M_o = 6.0$

$\alpha + \beta = 4°$

	Combustor Exit			Nozzle Exit			Afterbody		
	C_A	C_N	C_m	C_A	C_N	C_m	C_A	C_N	C_m
Hydrogen/Air $\phi = 1.0$	0.08309	-0.0056	-0.0076	0.093	C.0096	-0.011	-0.0050	0.016	-0.0044
Air (T = 311° K)	0.094	-0.006	-0.011	0.10	0.012	-0.013	-0.0040	0.013	-0.0035
58% Freon 13B1 + 42% argon	0.083	-0.0053	-0.0076	0.093	0.0095	-0.011	-0.005	0.016	-0.0044
40% Freon 12 + 60% argon	0.085	-0.0054	-0.0078	0.095	0.00973	-0.011	-0.0046	0.015	-0.0041

TABLE II.- BASIC EXTERNAL MODEL ASSEMBLY PARTS LIST

No.	Item	Model Stage					
		(a)	(b)	(c)	(d)	(e)	(f)
1	Forward fuselage	X	X	X	X	X	X
2	Aft fuselage and vertical tail	X				X	X
3	Full wings (LH and RH)	X				X	X
4	Stub wings (LH and RH)		X	X	X		
5	Flow-through scramjet modules block				X	X	
6	Flow-through scramjet modules off-block	X	X				
7	Forward fuselage fairing block	X	X		X	X	
8	Aft fuselage off-block		X	X	X		
9	Ramp plate	X				X	X
10	Blowing scramjet modules block			X			X
11	Blowing scramjet modules forward fairing block			X			X

TABLE III.- CANDIDATE FACILITIES FOR X-24C SCRAMJET TESTS

Facilities	Applicable Mach Range	Size	Type	(R/m) x 10^{-6}	Max R_∞ x 10^{-6}
1 LRC 20-in. hyp	6	0.51 x 0.51 m (0.41 m core)	Blow down (1 to 20 min)	2.3 - 30.5	25.7
2 LRC UPWT	3.0 - 4.6	1.2 x 1.2 m	Continuous	1.9 - 26.6	22.3
3 AMES 3.5-ft HWT	5 7	1.1 m dia (0.56 m core)	Blow down (0.25 to 4 min)	0.66 - 19.7 0.33 -26.2	11.1 14.7
4 AEDC Tun A	3 - 6	1 x 1 m	Continuous	0.98 - 14.1	19.8
5 AEDC Tun B	6 8	1.2 m dia	Continuous Continuous	1.64 - 10.2 2.3 - 12.1	14.2 17.0

TABLE IV.- PRELIMINARY TEST PROGRAM X-24C SCRAMJET SIMULATION

Run	M_∞	Configuration	α	Ψ	Gas Flow	Comments	Data Points	Repeat Points
1	6	(a) Complete vehicle no modules	-5 to +10	-5 to +5	No	Reference vehicle performance, Mode 1	12	3
2		(e) Complete vehicle with flow-through modules			No	Reference vehicle performance, Mode 2	12	3
3		(c) Truncated model with flow-through modules			No	Baseline increment, Mode3	12	3
4		(c) Truncated model with faired modules			No	Baseline increment, Mode 3	12	3
5	0	(d) Truncated model with blowing modules	0	0	Yes (3 values)	Static thrust calibration	3	6
6	6	(f) Complete vehicle with blowing modules	-5 to +10	-5 to +5	Yes (3 values)	Baseline increment, Mode 3	24	6
							75	24

TABLE V.- PREDICTED MODEL FORCES

X-24C 1/30-SCALE MODEL $M = 6.0$, $q = 55\ kN/m^2$, $\alpha + \beta = 4°$

Model Stage	Vehicle			Combustor Exit		
	F_A Kg (lb)	F_N Kg (lb)	My Nm (in. lb)	F_{3A} Kg (lb)	F_{3N} Kg (lb)	F_3My Nm (in. lb)
(a)	7.37 (16.25)	7.02 (15.47)	-0.60 (-5.34)	0	0	0
(b)	5.96 (13.15)	4.91 (10.83)	-0.48 (-4.27)	0	0	0
(c)	6.55 (14.43)	7.3 (16.09)	-0.48 (-4.27)	0	0	0
(d)	7.37 (16.25)	7.37 (16.25)	-3.90 (-34.50)	-18.36 (-40.47)	1.17 (2.57)	8.88 (78.58)
(e)	8.77 (19.34)	9.48 (20.89)	-4.02 (-35.59)	-18.36 (-40.47)	1.17 (2.57)	8.88 (78.58)
(f) (ϕ = 1.0)	-26.57 (-58.58)	14.2 (31.40)	13.28 (117.51)	-29.09 (-64.14)	-1.86 (-4.08)	15.33 (135.70)
(Flight ϕ = 1.0)	-7.39 (-16.29)	13.15 (28.99)	0.98 (8.70)	-	-	-
Normal rated load of balance	$\pm$31.75 ($\pm$70)	$\pm$54.4 ($\pm$120)	$\pm$16.95 ($\pm$150)	F(flight ϕ=1) = F(f)-F(c)+F(d)-F_3(d)		
Balance accuracy (design spec)	$\pm$0.164 ($\pm$0.14	$\pm$0.109 ($\pm$0.24)	$\pm$0.034 ($\pm$0.30)			

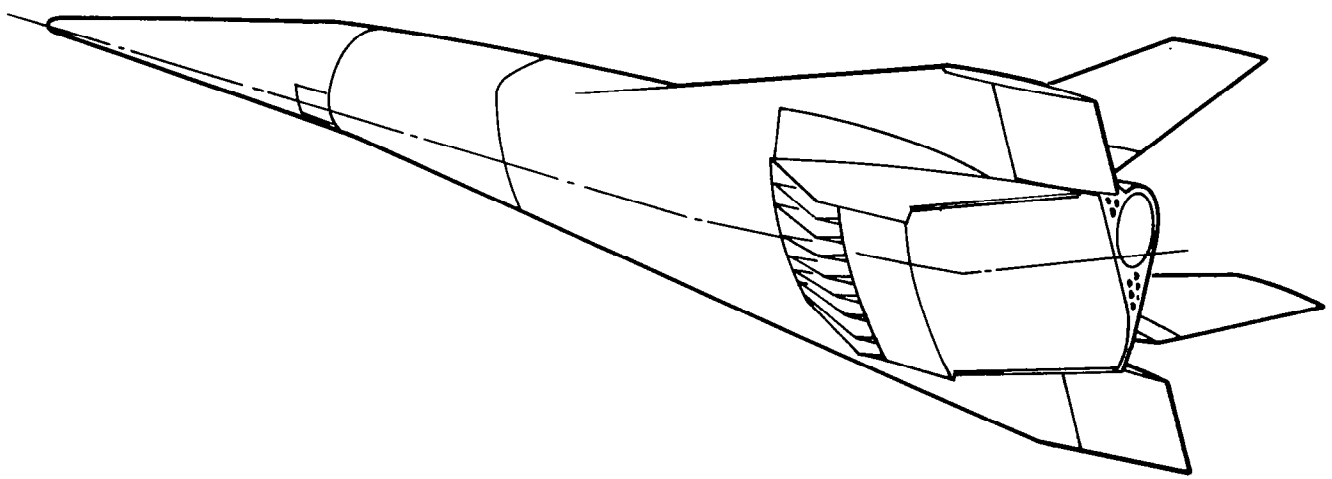

Figure 1.- NASA/USAF high-speed research airplane (X-24C).

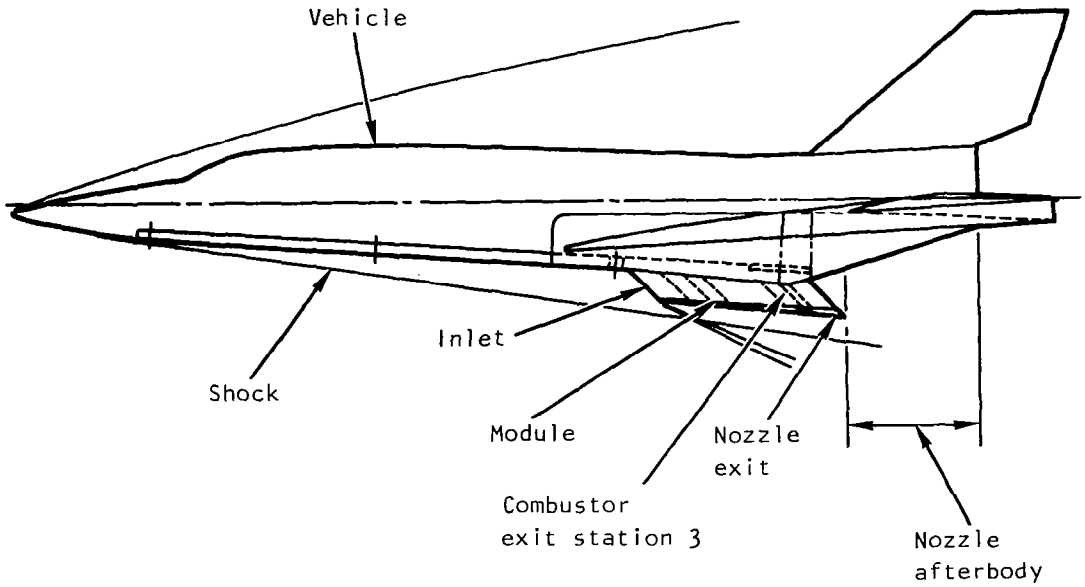

Vehicle forces

- Clean vehicle forces (no modules)
- Deduct forces on vehicle subtended by modules & nozzle
- Related moments

Propulsion forces

- Inlet momentum
- Combustor exit momentum
- Nozzle expansion surfaces (upper & lower)
- Module cowl external forces
- Inlet spillage forces
- Related moments

Figure 2.- Vehicle and propulsion forces.

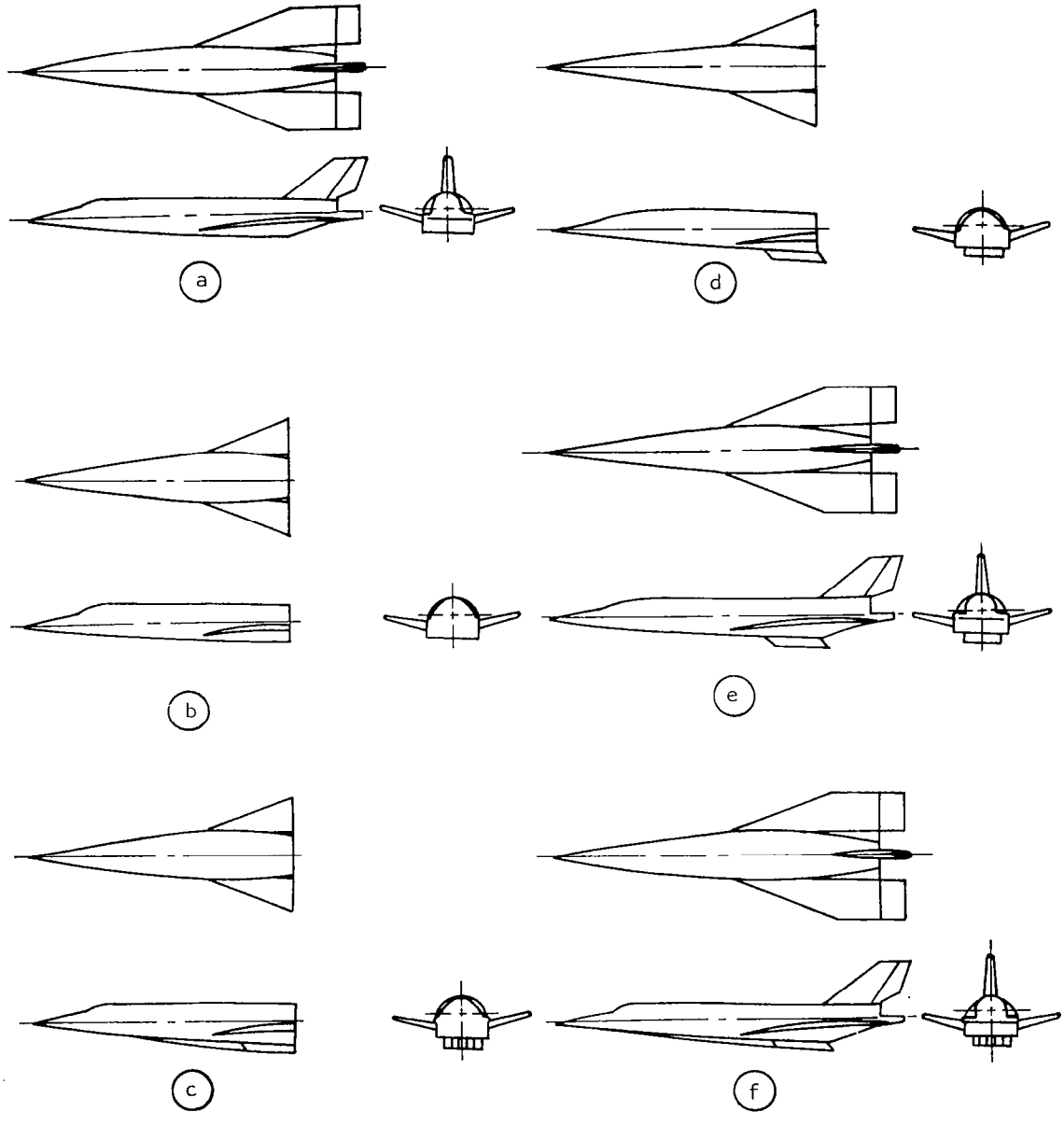

Figure 3.- Force accounting model stage configurations.

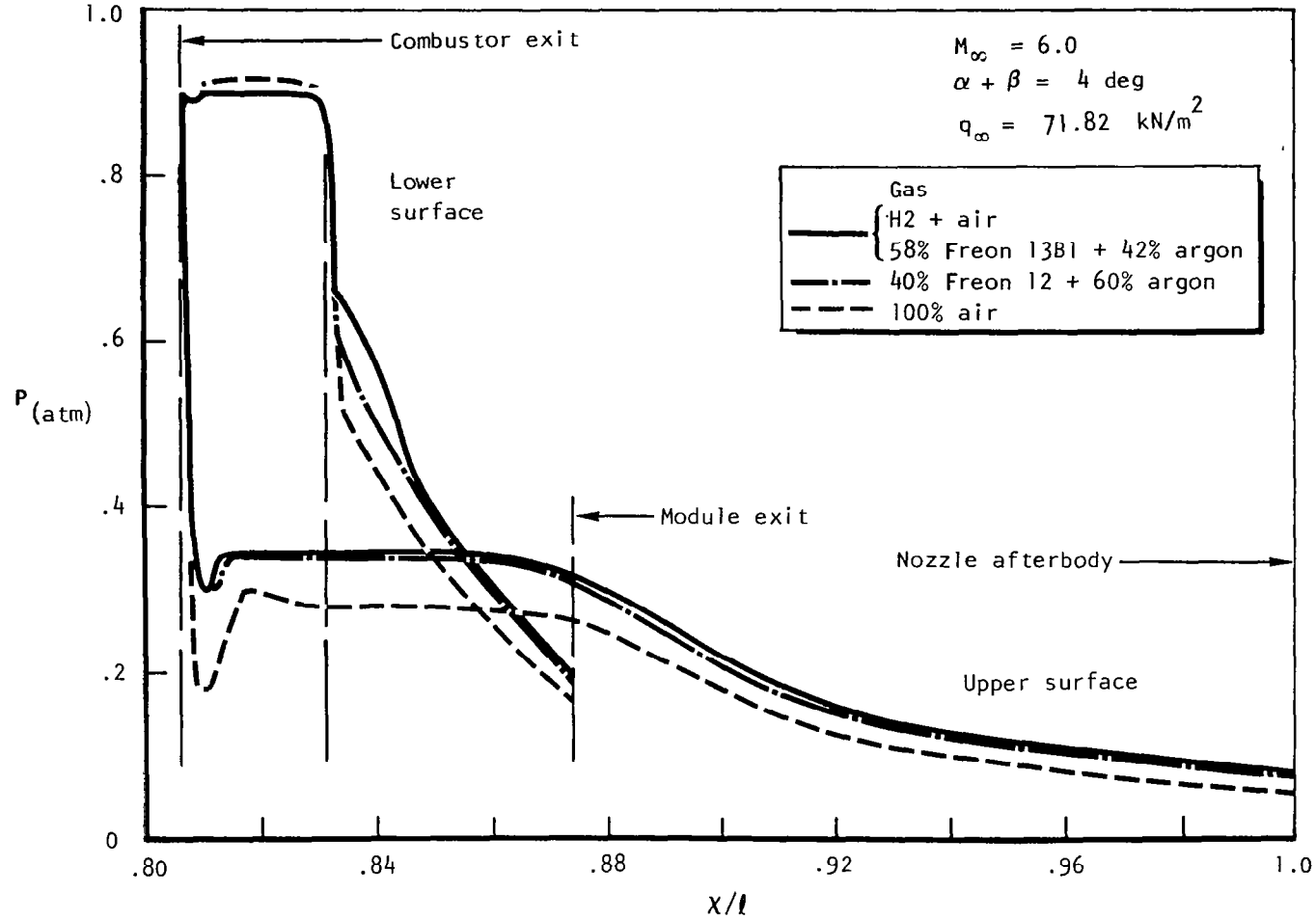

Figure 4.- Exhaust gas simulation effectiveness - nozzle surface pressures.

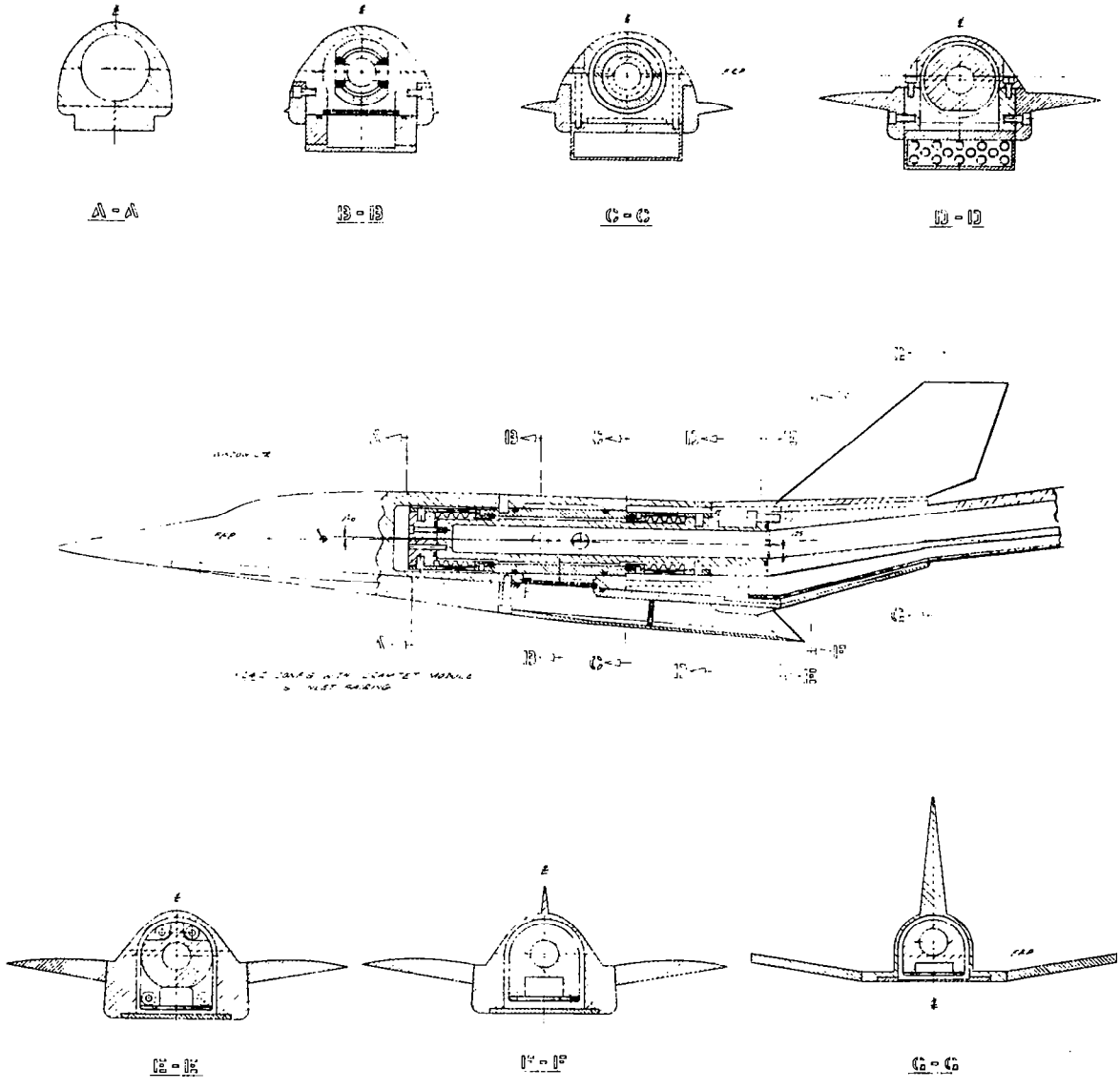

Figure 5. - 1/3-scale basic model X-24C scramjet simulation test.

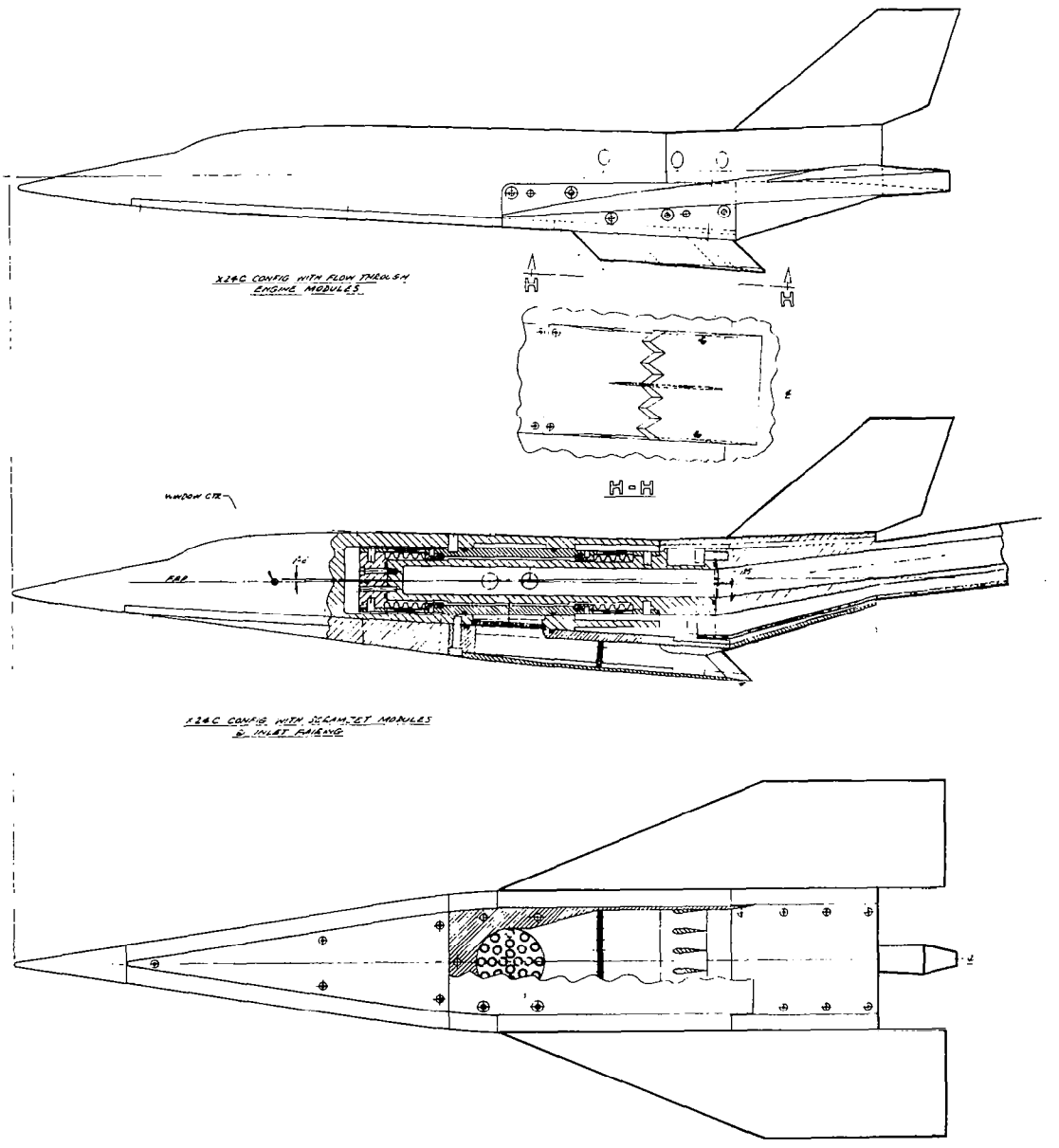

Figure 5. - Continued.

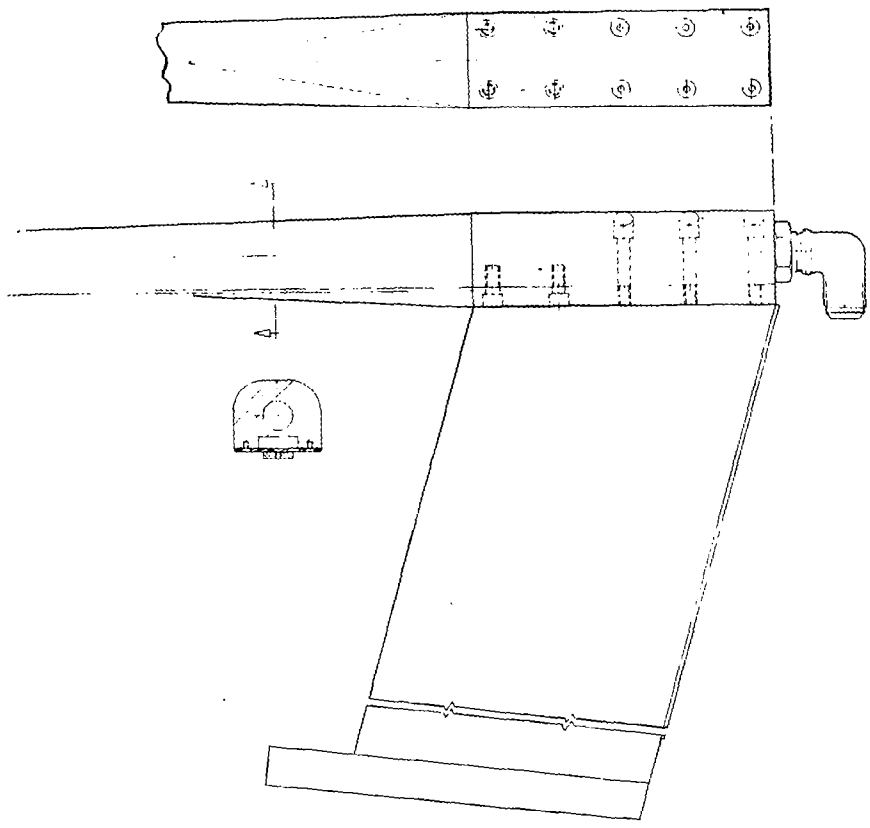

Figure 5. - Concluded.

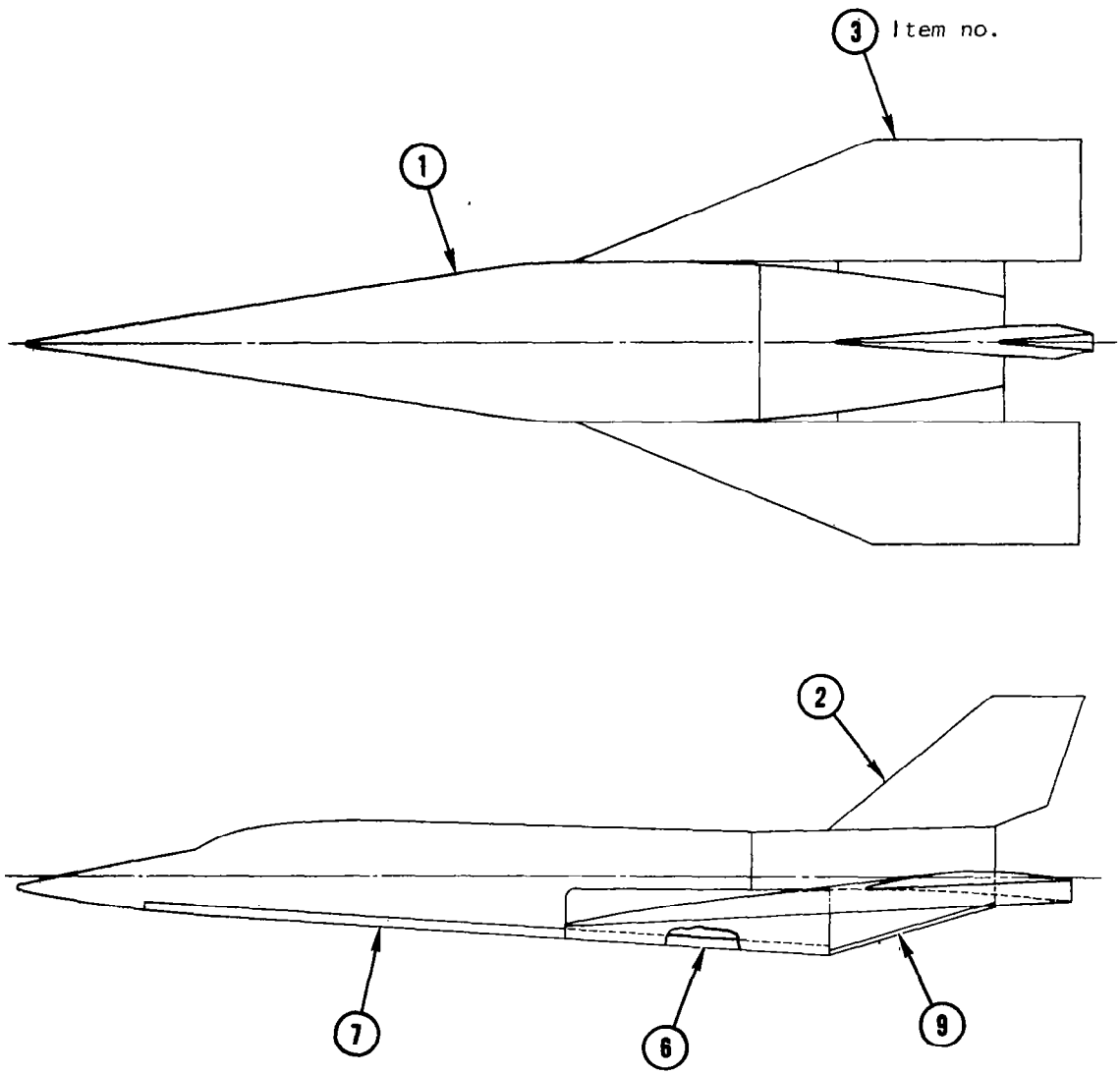

Configuration (a)

Figure 6.- X-24C scramjet simulation test model stage definition.

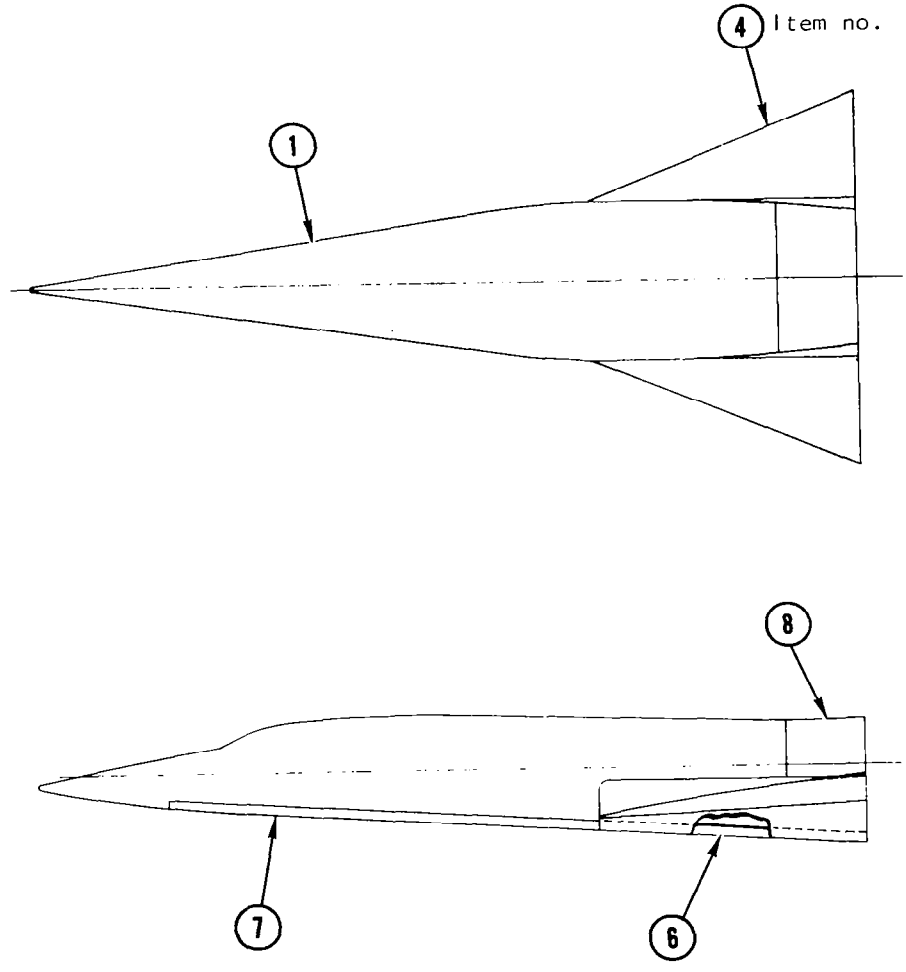

Configuration (b)

Figure 6.- Continued.

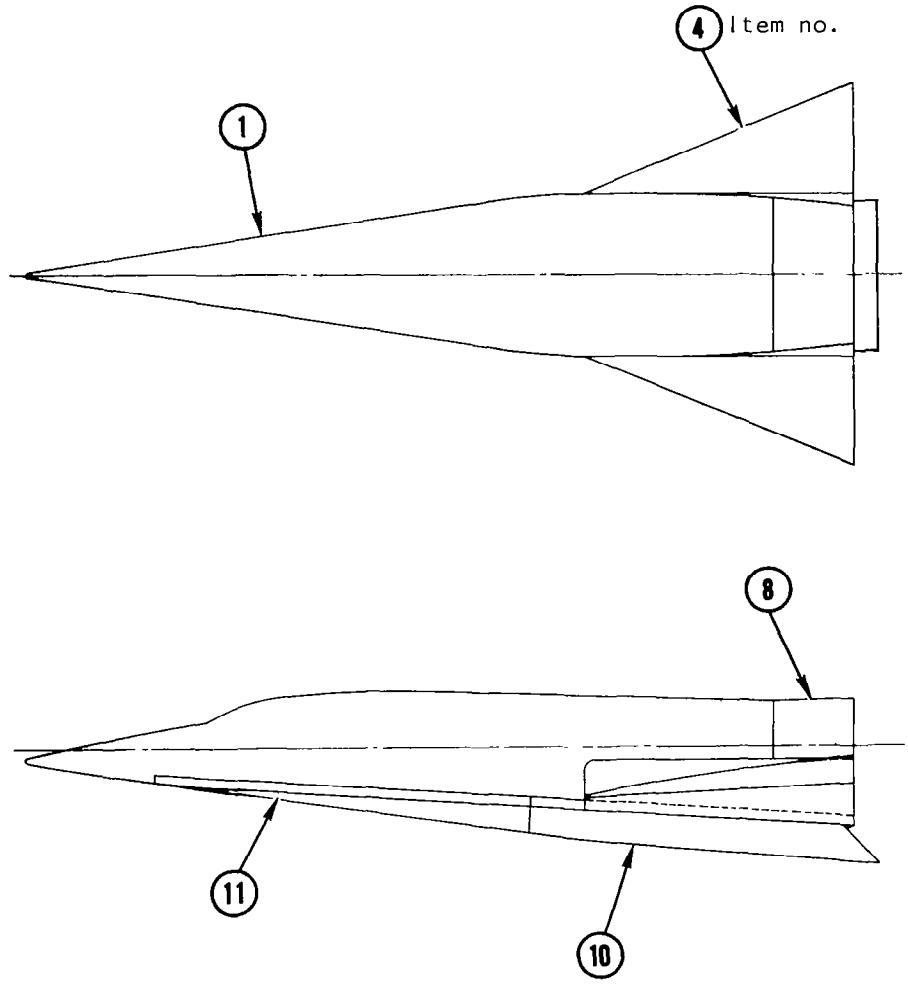

Configration (c)

Figure 6.- Continued.

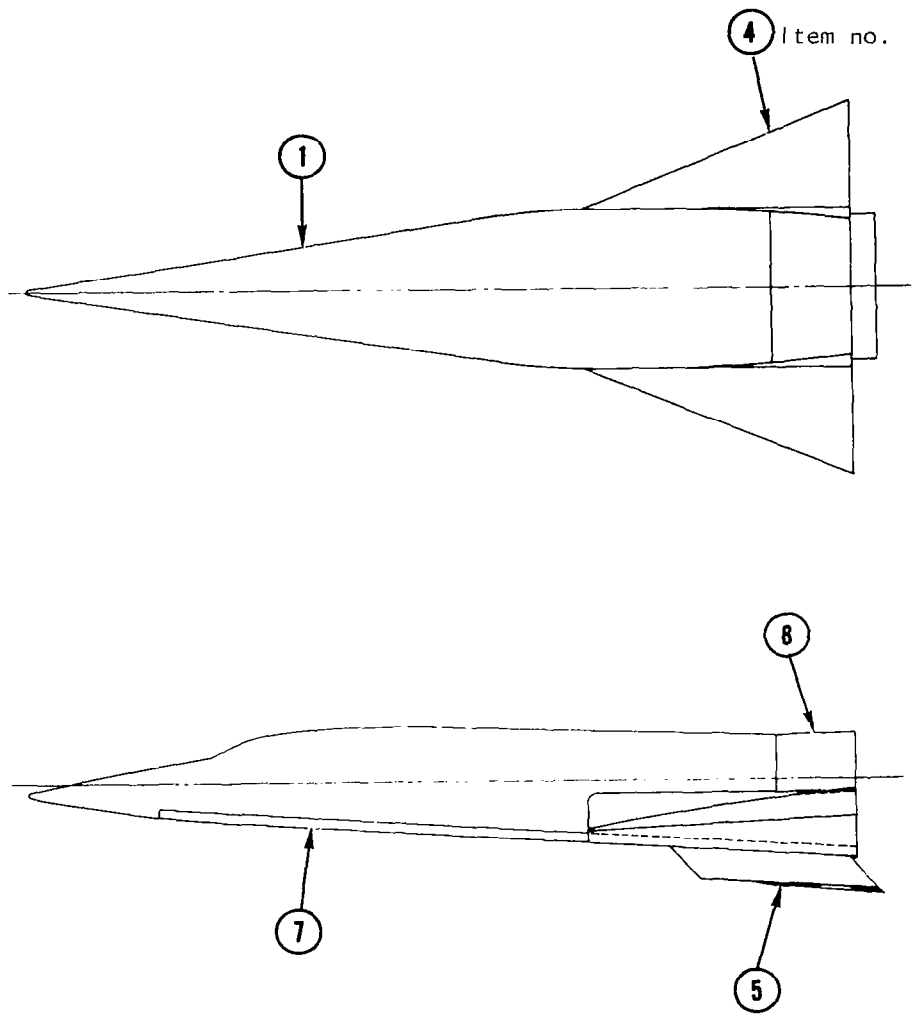

Configuration (d)

Figure 6.- Continued.

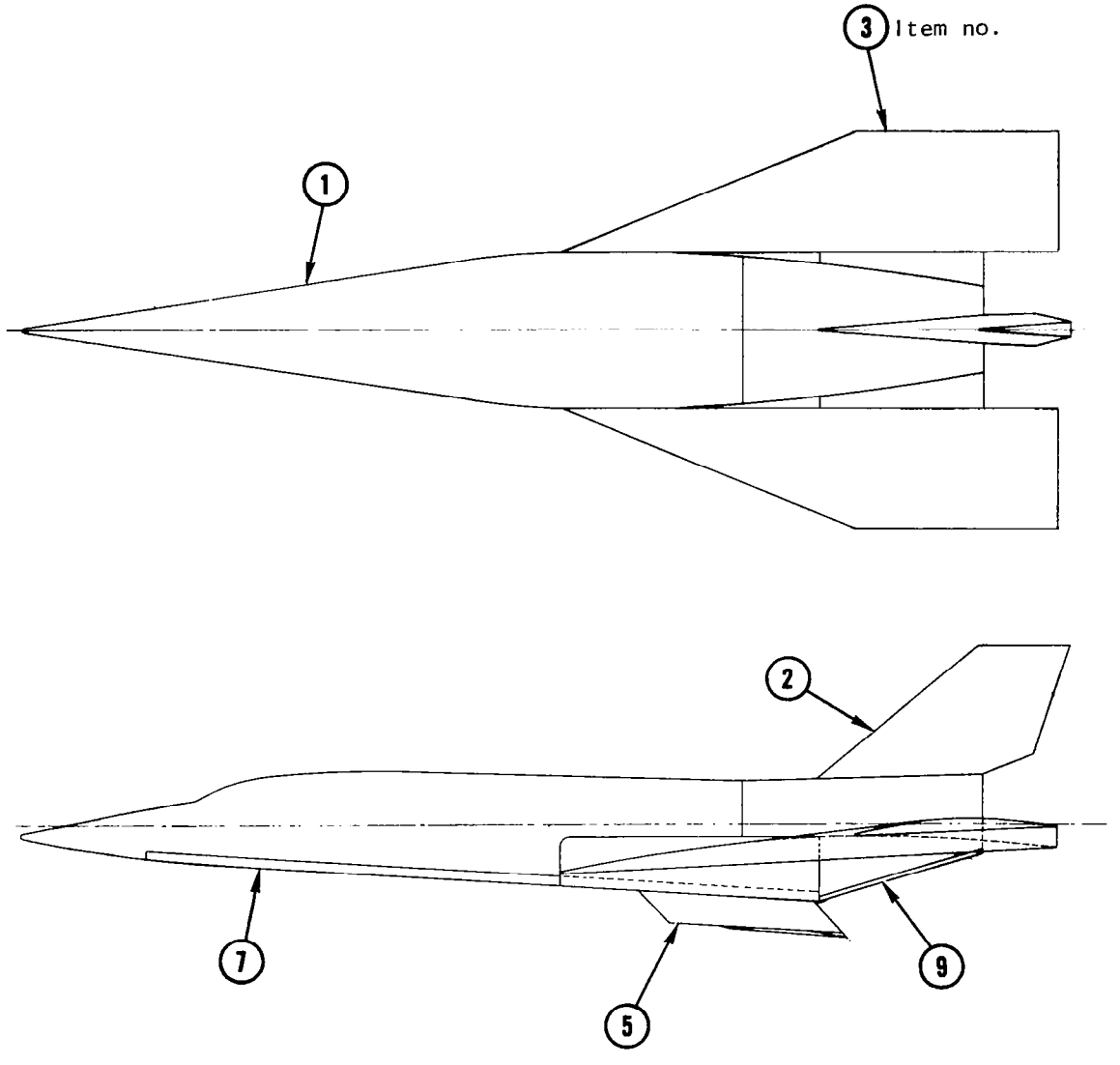

Configuration (e)

Figure 6.- Continued.

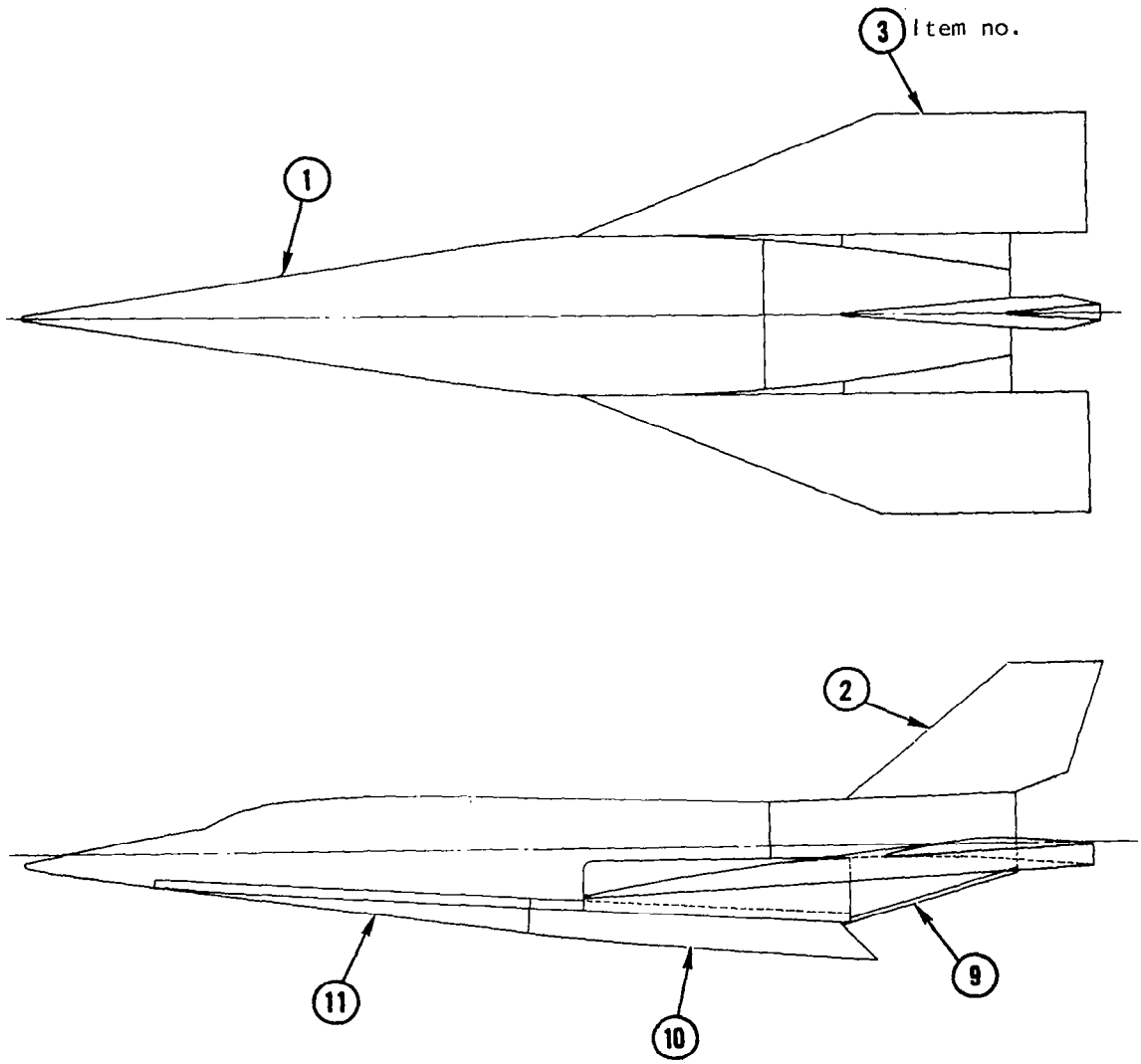

Configuration (f)

Figure 6.- Concluded.

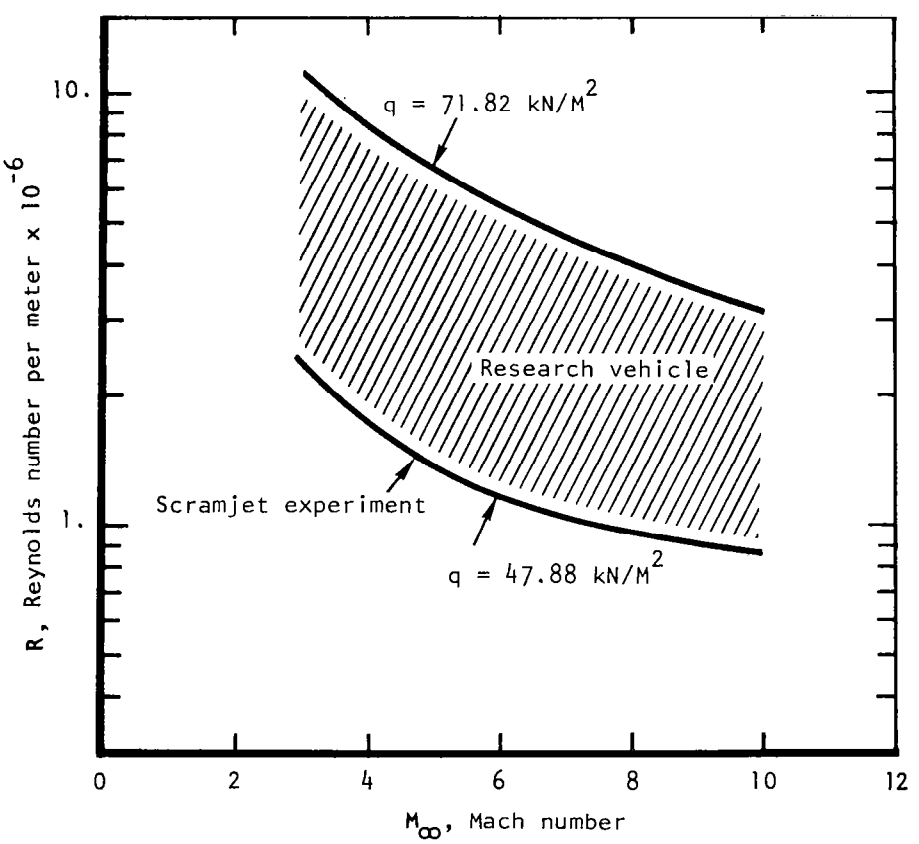

Figure 7.- Reynolds number - Mach number regime X-24C.

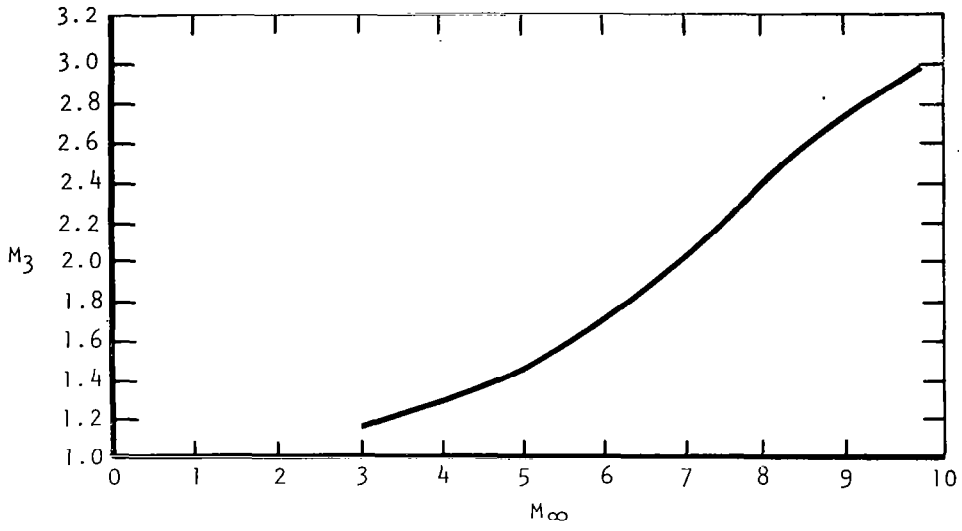

Figure 8.- Combustor exit plane Mach number, M_3.

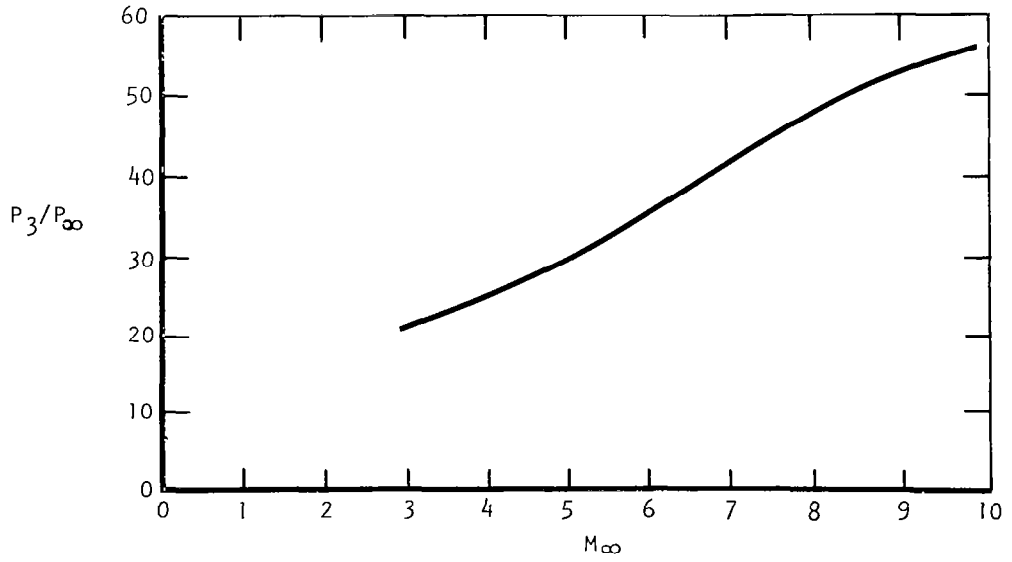

Figure 9. - Combustor exit pressure ratio, P_3/P_∞.

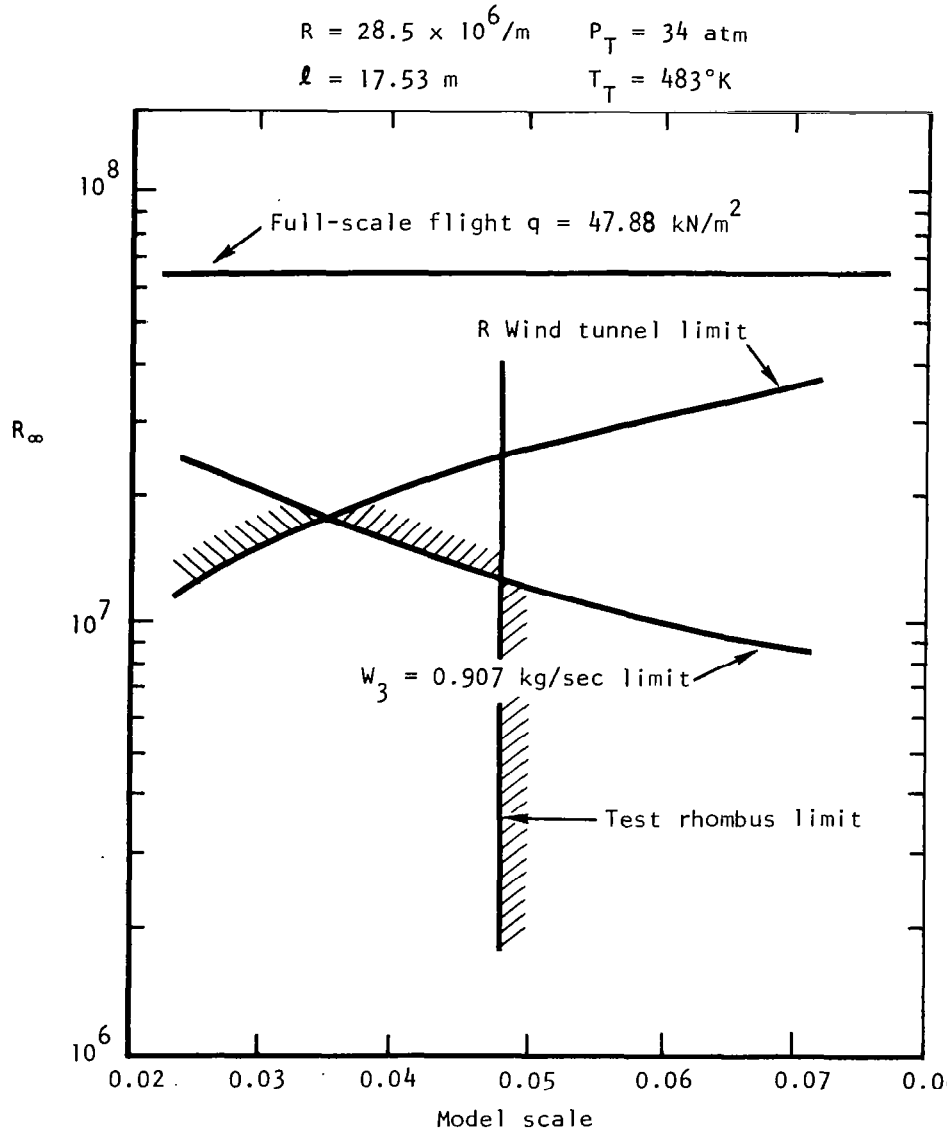

Figure 10.- Model scale limits NASA LRC 20-inch Mach 6 wind tunnel.

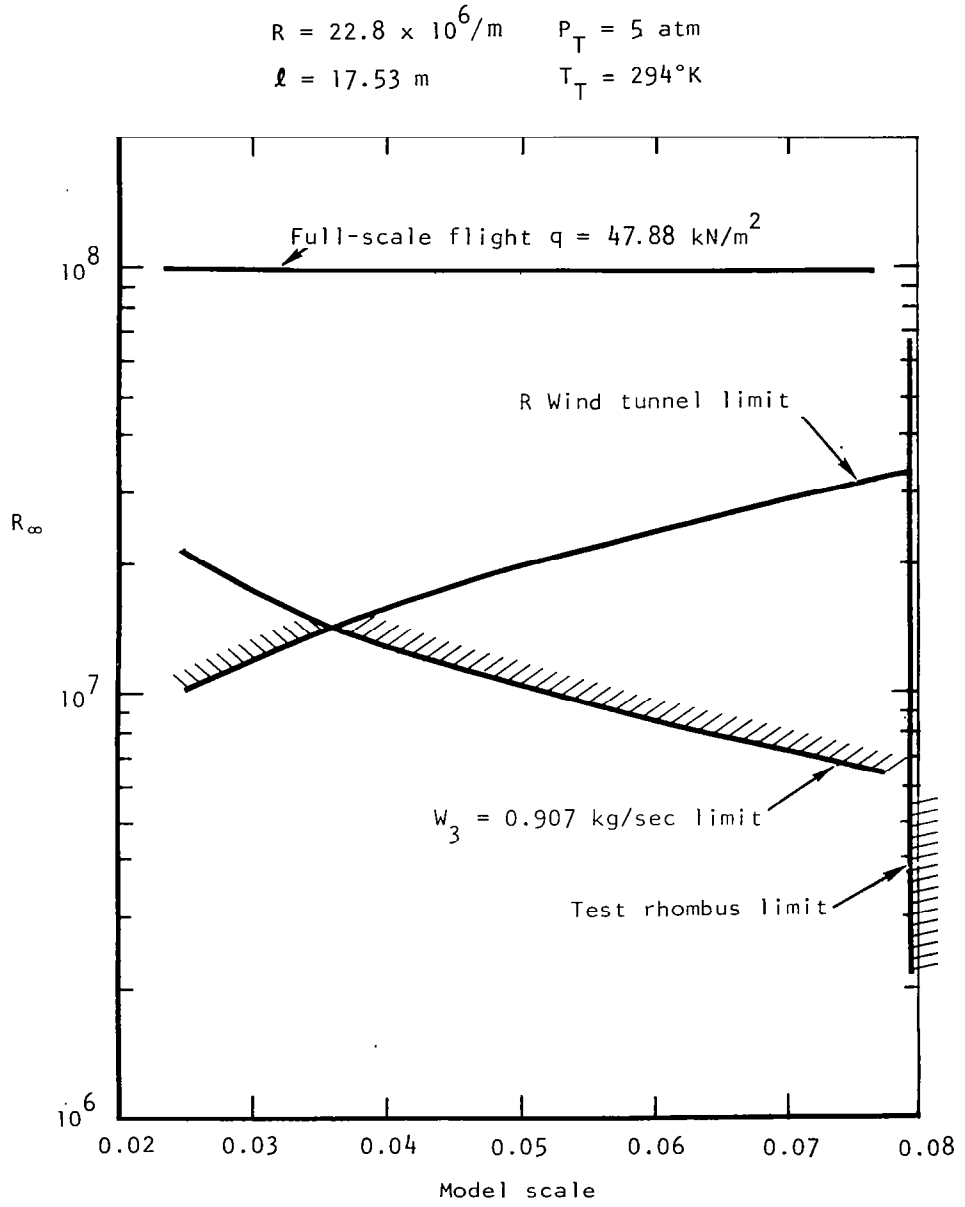

Figure 11.- Model scale limits AEDC VKF tunnel A at Mach 4.0.

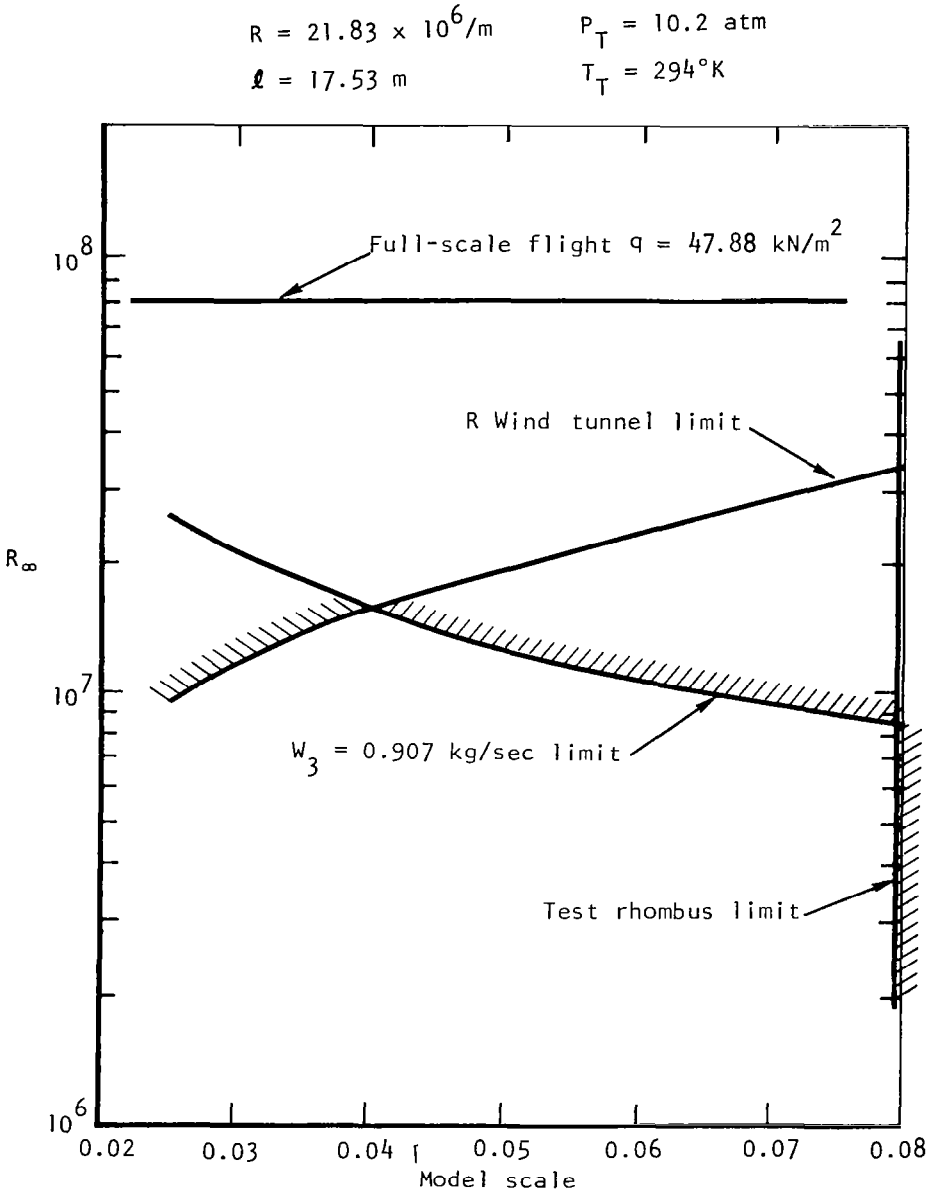

Figure 12.- Model scale limits AEDC VKF tunnel A at Mach 5.0.

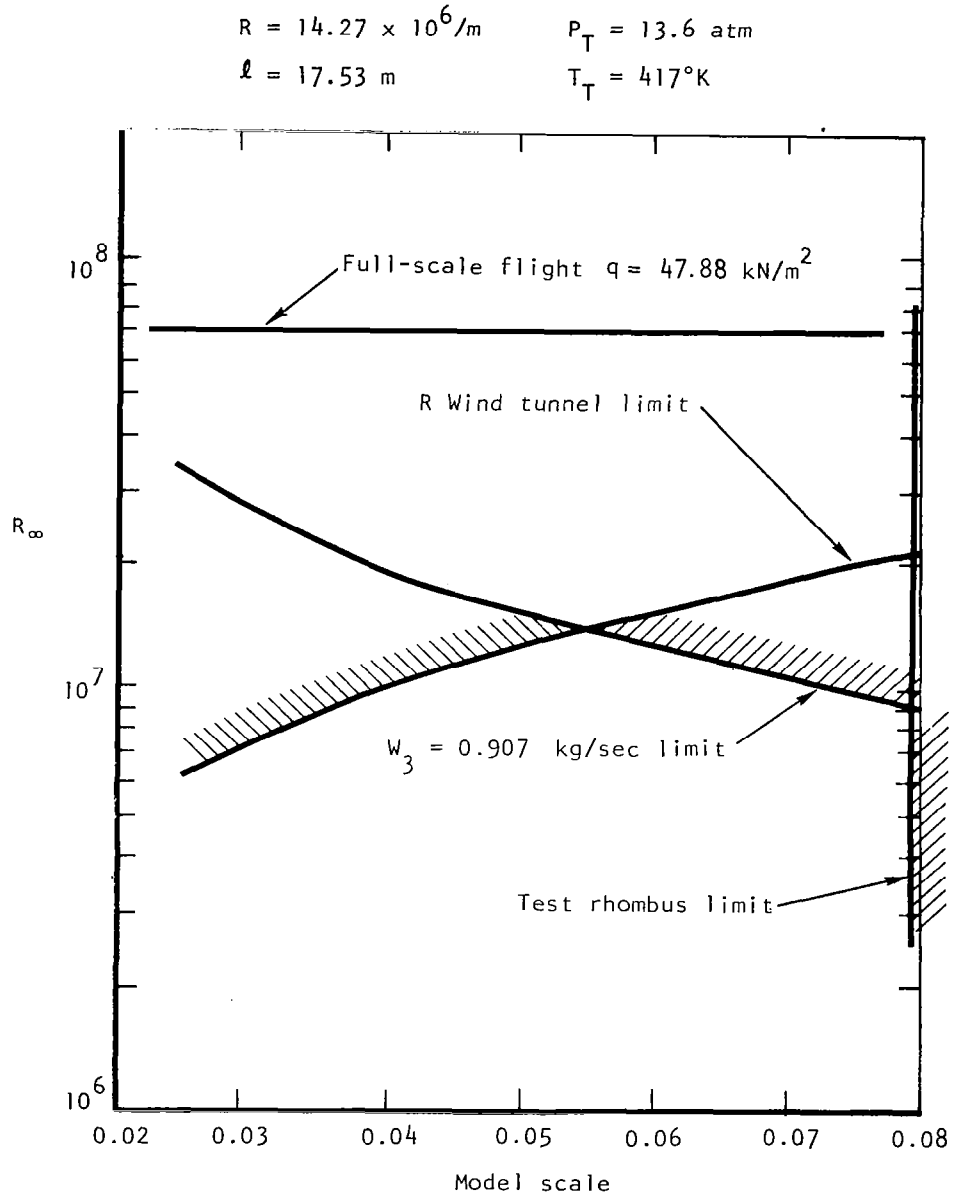

Figure 13.- Model scale limits AEDC VKF tunnel A at Mach 6.0

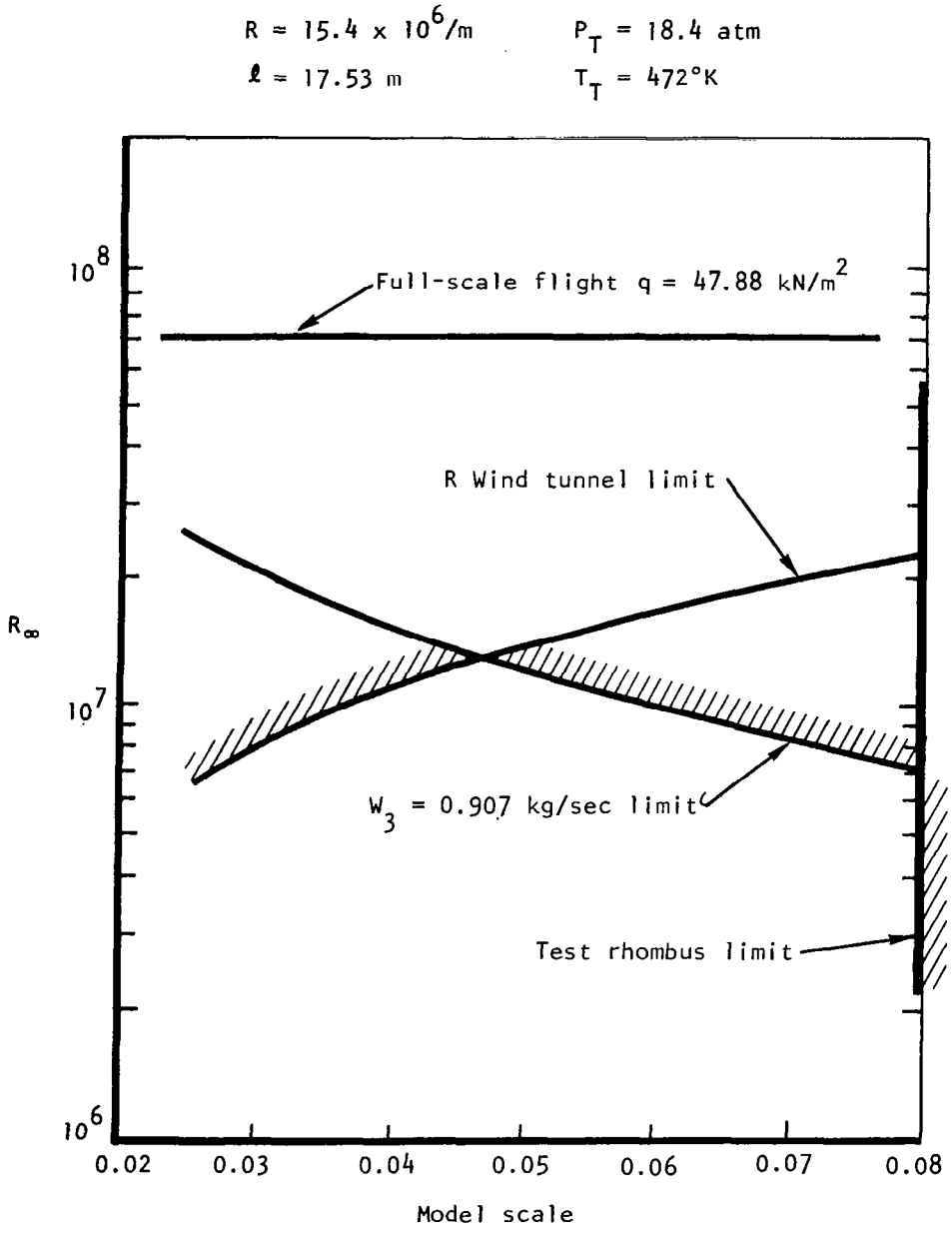

Figure 14.- Model scale limits AEDC VKF 50-inch tunnel at Mach 6.0.

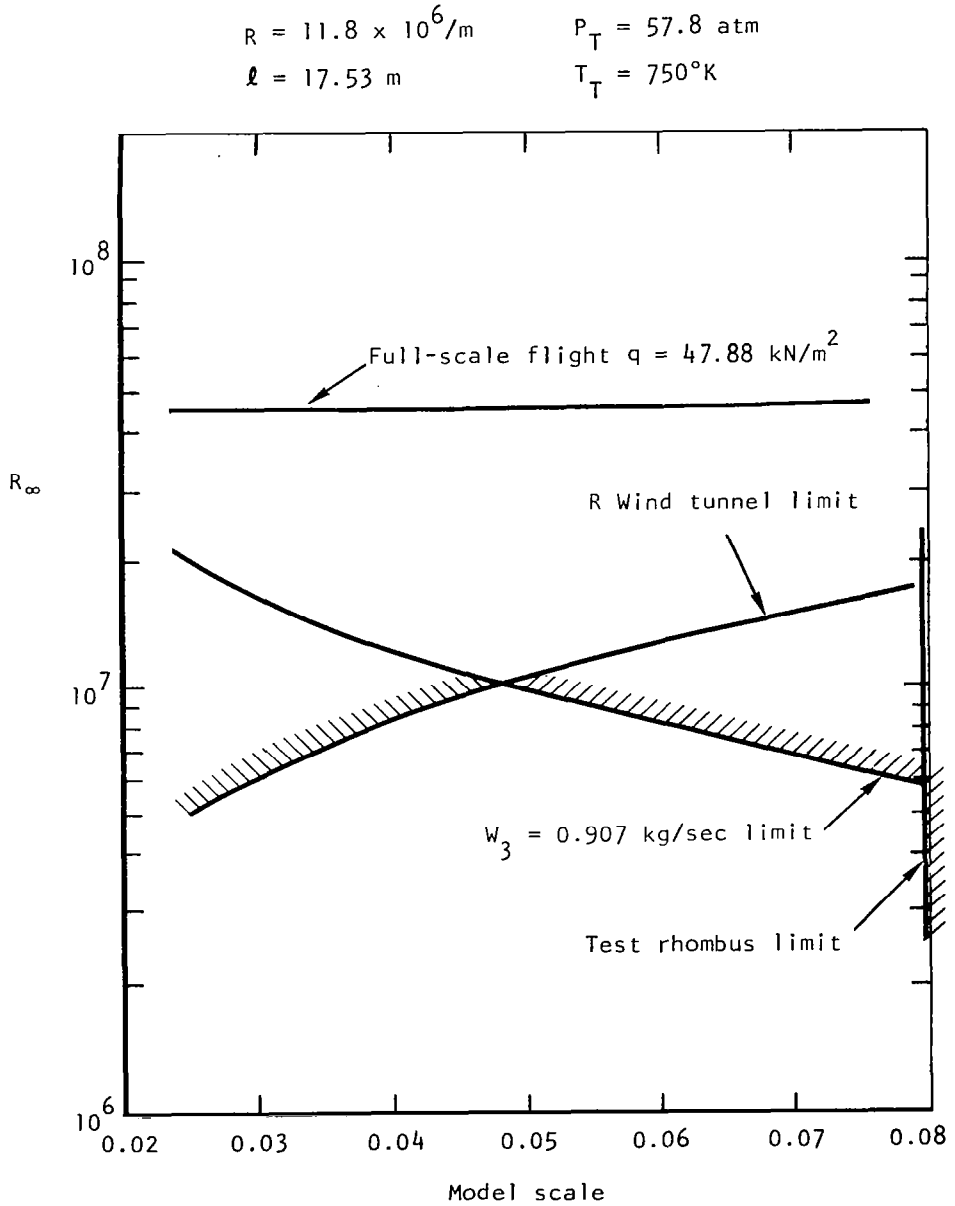

Figure 15.- Model scale limits AEDC VKF 50 inch-tunnel at Mach 8.0.

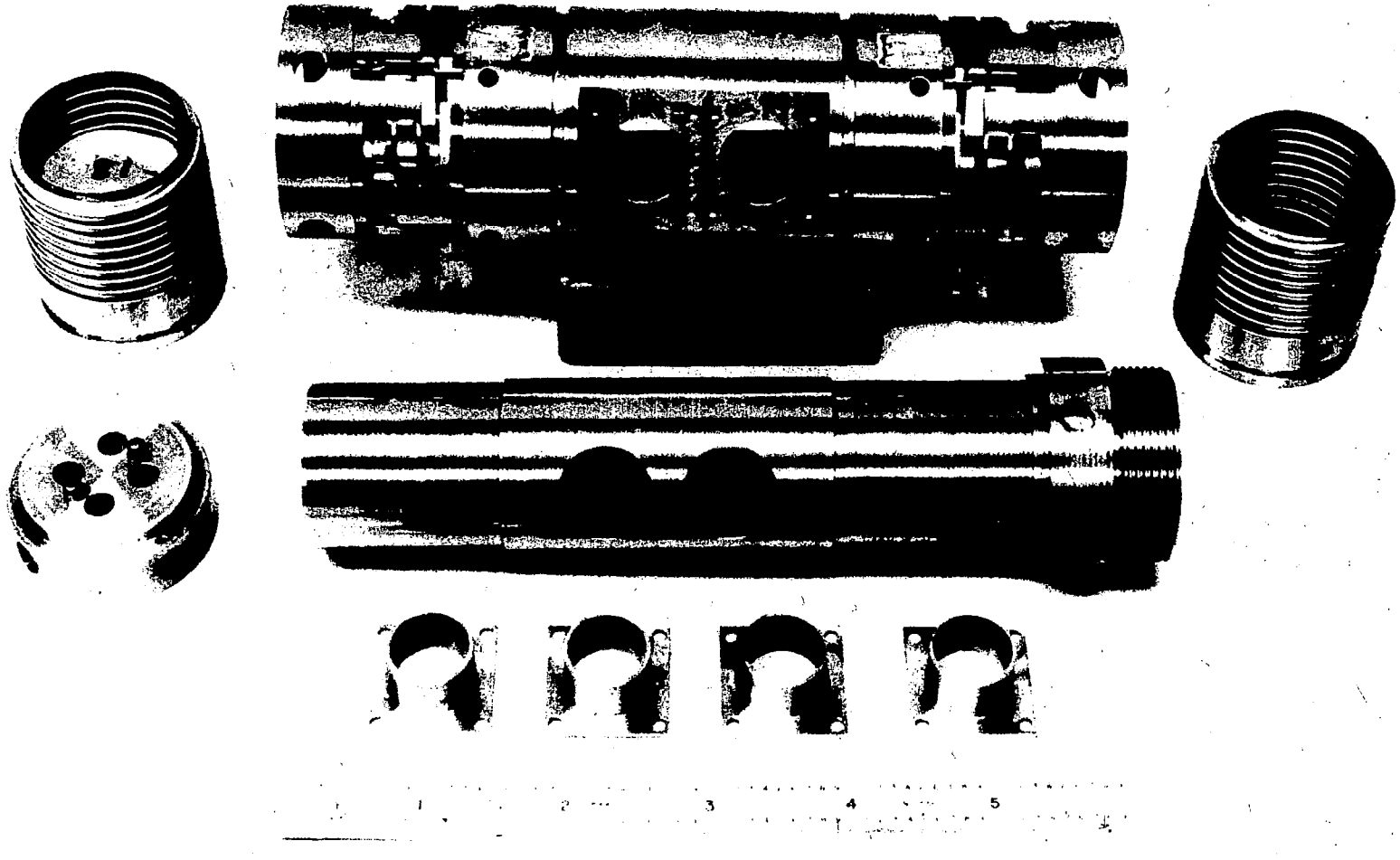

Figure 16.- Six component flow-through balance.

APPENDIX

SPECIFICATION FOR A FLOW-THROUGH FORCE BALANCE FOR THE 1/30-SCALE X24C-L16 WIND TUNNEL MODEL

Prepared By: G. A. Wilhelm

BASIC SPECIFICATIONS

TABLE OF CONTENTS

1.0 SCOPE

1.1 This specification defines the requirements for design and calibration of a flow-through six-component strain gaged balance that will be used to measure aerodynamic and thrust loads on a 1/30-scale wind tunnel model of the X24C-L16 hypersonic research aircraft. The balance is to be used for this specific purpose and compromises for broad range usage should not be considered.

2.0 PROBLEM

2.1 The X24C program has as one of its prime objectives, the role of test bed for integrated SCRAMJET engines. The subject wind tunnel model will be used to provide predictions of vehicle performance with the interactive effects of these engines simulated by using substitute gases to replace the complex gases existing in the actual SCRAMJET exhaust flow. The substitute or simulant gas will be plumbed through the support sting and force balance, with the flow exiting the balance perpendicular to the axial force direction, and with the exits in an opposed arrangement to minimize flow momentum effects. The flow dumps into an annular plenum and routes to the SCRAMJET engine modules. The simulant gas mixture will consist of either 40 percent Freon 12 + 60 percent Argon or 50 percent Freon 13B1 + 50 percent Argon and will be restricted to the following conditions: maximum flow rate of 2.0 pounds per second, maximum stagnation pressure of 250 psia, and maximum stagnation temperature of 500°F. The problem lies in routing the simulant gas onboard the model without causing balance tare loads that are large in comparison to model aerodynamic loads, and in minimizing tare loads that are functions of temperature, pressure, and flow rate, and other variables that are difficult to compensate and calibrate.

2.2 Inadvertent breakdown of the freestream flow in the Langley Research Center 20-inch Hypersonic Wind Tunnel would subject the force balance to dynamic loads that are several times larger than the expected steady state running loads. The balance strain gaged sections should be stressed to obtain the most accurate measurement of the steady state loads, however, the balance should also be designed to insure model survival during a flow breakdown condition.

2.3 Six components will be measured: forward normal force (N1), aft normal force (N2), axial force (A), forward side force (Y1), aft side force (Y2), and rolling moment (ℓ).

2.4 The balance must be capable of measuring the calibration loads (Section 9.1) at the accuracy, repeatability, and hysteresis levels specified in sections 7.1 and 7.2.

3.0 BACKGROUND

3.1 Hypersonic vehicles with SCRAMJET propulsion systems present a number of complications for research and development of conceptual designs in wind tunnel tests. Configurations currently under study feature integration of the SCRAMJET nozzle expansion surface into a large portion of the vehicle lower aft surface. The expansion of the engine exhaust gases can generate forces and moments which approach, in magnitude, the aerodynamic forces and moments of the vehicle without exhaust flow. Since use of the actual gases (hydrogen and air) does not lend itself to direct duplication of the supersonic combustion process for scaled wind tunnel models, a study was conducted to propose a substitute or simulant gas mixture which would best match the desired pressure distribution on the model afterbody/nozzle. As a result of this study, binary mixtures of Freon and Argon gas, with stagnation temperature to 500°F, were selected to give an accurate simulation of the pressure distributions.

4.0 OBJECTIVES

4.1 The objective of this specification is to expedite the design and manufacture of a six-component force balance for measuring external aerodynamic loads combined with simulated engine exhaust loads on a 1/30-scale wind tunnel model of the X24C-L16 hypersonic research aircraft. The balance should meet the requirements for size, capacity, rigidity, and accuracy as set forth in this specification.

5.0 DESIGN CONSIDERATION

5.1 Dimensions

5.1.1 The maximum diameter of the balance should not exceed 1.9 inches. The aft face of the balance outer sleeve will be

located at model station 18.0 inches (which is 3.07 inches aft of the estimated normal force center of pressure). Normal force gage spacing should be from 4.0 to 5.5 inches. The inside diameter of the simulant gas passageway through the sting and balance tube shall not be less than 0.75 inches (preferably larger).

5.2 Load Capacity

5.2.1 The normal rated loads for the design of the balance are based on the maximum running loads at the model moment reference center (Fuselage reference line at model station 14.96 inches). These loads are:

Component	Running Load	Normal Rated Load
Normal Force	+112. lbs.	±120. lbs
Axial Force	-70. to +19. lbs	±70. lbs
Side Force	±44. lbs.	±50. lbs
Pitching Moment	-59. to +133. in-lbs.	±150. in-lbs.
Yawing Moment	±43. in-lbs.	± 50 in-lbs.
Rolling Moment	±64. in-lbs.	± 75. in-lbs.

5.2.2 The flow breakdown loads are based on Langley Research Center 20-inch Hypersonic Wind Tunnel design criteria. The normal, axial, and side forces are applied at the centroid of the model planform, frontal, and side areas, respectively. Rolling moment is applied about the balance centerline. The normal and side force do not occur simultaneously. These loads are:

Component	Flow Breakdown Load
Normal Force	±935. pounds
Axial Force	±195. pounds
Side Force	±455. pounds
Rolling Moment	±910. inch-pounds

5.3 Safety Factors

5.3.1 The balance shall be capable of measuring the normal rated loads (Section 6.2.1) of any or all types, singly or simultaneously, in either direction, with a factor of safety 3.0, based on the yield strength of the material.

5.3.2 The balance shall be capable of withstanding the flow breakdown loads as defined in Section 6.2.2. The normal and side force do not occur simultaneously. A factor of safety 1.0, based on the yield strength of the material, is required.

5.3.3 All screws, pins, and other fastening devices shall have a factor of safety 4.0, based on the yield strength of the material.

5.4 Deflections

5.4.1 Deflections shall not exceed 0.5 degree when maximum rated loads are applied simultaneously in opposite directions on forward and aft normal force or on forward and aft side force. This value includes the deflection in the joint at the sting attachment.

5.4.2 Deflection due to rolling moment shall not exceed 0.25 degrees when maximum rated rolling moment is applied to the balance.

5.5 Thermocouples

5.5.1 The balance will be instrumented with one chromel-constantan thermocouple located near each strain gage bridge, and with one chromel-constantan shielded total temperature probe located in the gas flow passageway. The thermocouples are to be installed on the non-metric side of the balance.

5.6 Pressures

5.6.1 The balance gas flow passageway will be instrumented with two static pressure orifices utilizing 0.042" O.D. stainless steel tubing, and one total pressure probe.

5.7 Electrical Leads

5.7.1 All balance strain gage and thermocouple leads will exit the model via the non-metric inner tube. Each strain gage bridge will have six wires: two each for input, output, and reference voltage.

5.7.2 The electrical leads shall be 35 feet long with no splices. The strain gage leads shall be no smaller than 34 gage wire and no larger than 30 gage wire, with minimum insulation thickness. The electrical wires will be sheathed into a cable of 0.25 inch maximum diameter. The cable shall be constructed so that the sheathing and not the wires, will carry the tension load experienced during installation and handling.

5.7.3 The following color code will be used for the balance bridges:

Gage Comp.	No. Code	Input		Output		Voltage Measurement	
		Pos.	Neg.	Pos.	Neg.	Pos.	Neg.
N_1	1	Red	Black	Green	Blue	White & Red	White & Black
N_2	2	Red	Black	Green	White	"	"
A_{fwd}	3_F	Red	Black	Green	Purple	"	"
A_{aft}	3_A	Red	Black	Green	White & Purple	"	"
Y_1	4	Red	Black	Green	Gray	"	"
Y_2	5	Red	Black	Green	Yellow	"	"
ℓ_{fwd}	6_F	Red	Black	Green	Orange	"	"
ℓ_{aft}	6_A	Red	Black	Green	White & Orange	"	"

NOTE: If red wire with a white stripe and black wire with a white stripe are not available, it is acceptable to use solid colors for the voltage measurement wires.

5.7.4 All thermocouples shall utilize certified thermocouple wire and each shall be identified numerically.

5.0 DESIGN CONSIDERATION - Continued

5.8 Simulant Gas Flow Requirement

5.8.1 The balance shall provide flow-through capability for various mixtures of Freon and Argon gas at the following conditions: maximum flow rate of 2.0 pounds per second, maximum stagnation pressure of 250. psia, and maximum stagnation temperature of 500°F. Based on the 0.75 inch minimum flow diameter, the duct Mach number will be 0.3. Fabrication of the internal flow duct and the support sting from a single piece of material would be desirable, although not a necessity. If the method of balance support includes a joint at the sting attachment, the pressure seal design must insure no loss of simulant gas flow.

5.9 Balance Temperature Stability

5.9.1 The temperature of the balance during operation in the Langley 20-inch HWT will be determined by: the temperature of the wind tunnel freestream flow (adiabatic wall temperature equals 515°F based on M = 6, and T_T = 1080°R), the temperature of the simulant gas flow (adiabatic wall temperature equals 490°F based on M = 0.3, and T_T = 960°R), and the duration of the wind tunnel run time. Actual temperatures will not exceed the above values.

5.9.2 Consideration should be given to methods for installing heating elements into the balance and sting so that the strain gaged sections could be preheated to an equilibrium temperature representative of the operationally induced temperatures. Also, methods for insulating the balance should be suggested.

6.0 PERFORMANCE

6.1 Accuracy

6.1.1 All loadings on a single balance component shall produce data which does not deviate more than 0.2% of the normal rated load from the best straight line fit through the data points.

6.1.2 Furthermore, all loadings on a single balance element shall produce data which does not deviate more than 0.1% of the normal rated load from the best second degree curve fit through the data points for positive and negative loadings taken separately.

6.1.3 These accuracy values (Sections 7.1.1 and 7.1.2) are for the completely assembled balance and include force and moment interactions but do not include corrections for pressure, flow rate, or temperature gradients.

6.1.4 Accuracies are quoted for positive and negative loadings made during separate runs.

6.1.5 When a single type load is gradually applied to the design value (Section 6.2.1), then gradually unloaded to zero, the data produced in the range from zero to the calibration load (Section 9.0), and back, shall fall within the limits specified in Sections 7.1.1, 7.1.2, 7.1.3, and 7.1.4.

6.1.6 Pressure and gas flow calibration runs shall produce data which does not deviate more than ±0.3% from the best straight line fit through the data.

6.2 Hysteresis

6.2.1 The hysteresis of any bridge output reading, for any single series of loadings, from zero to the normal rated load for that individual bridge, shall be within 0.1% of the bridge output at normal rated load.

6.2.2 The hysteresis of any bridge output reading, for a temperature excursion from 60°F to 460°, shall be within 0.25% of the bridge output at normal rated load.

6.3 Repeatability

6.3.1 The repeatability of the balance shall be within the accuracy requirements noted in Section 7.1. The repeatability shall be demonstrated by comparing data measured at the same conditions before and after cycling a component through a full cycle of positive and negative loads.

6.4 Interactions

6.4.1 The interaction on any component caused by the application of normal rated load on any other component will be within the following values: The interactions on axial force due to all components except rolling moment will be within 1%. The interaction of rolling moment on axial force will be within 2%. The interactions on forward normal force and aft normal force will be within 4%. The interactions on all other components will be within 2%.

6.4.2 The interaction data shall be linear within 20% of the maximum allowable interaction values, and shall be smooth regular data, capable of being fitted within straight line or second degree curves. The deviation of the data from the straight line or second degree curve shall be within the accuracy limits specified in Section 7.1.

6.5 Sensitivity

6.5.1 The bridge sensitivity shall be equal to or greater than the values listed below without benefit of external amplification. These sensitivities are to be obtained by using strain gages with a gage factor of 4.5 (92% Platinum - 8% Tungsten) and a stress level of 7500 psi, broad operating temperature range (-320°F to +1000°F), high output (gage factor 4.5), superior hysteresis characteristics, and automatic modulus compensation on steel.

COMPONENT	BRIDGE OUTPUT AT NORMAL RATED LOAD
N1	1.2 mv/v
N2	1.2 mv/v
A	1.2 mv/v
Y1	1.2 mv/v
Y2	1.2 mv/v
ℓ	1.2 mv/v

6.0 PERFORMANCE

6.6 Temperature Stability

6.61 The change of sensitivity of any component bridge shall not exceed 0.5% per 100°F due to temperature changes in the range from 60°F to 460°F. This effect should be checked at a minimum of three stabilized temperatures within the temperature range.

6.6.2 The zero shift due to temperature changes within this range shall be less than 1.0% of the bridge output at normal rated load.

7.0 STRAIN GAGE CHARACTERISTICS

7.1 Operating Voltage: The maximum operating voltages for all bridges shall be at least 18 volts.

7.2 Bridge Resistance: The bridges shall utilize high temperature 350 ohm strain gages.

7.3 Gage Factor: The gage factor shall be 4.5 for all bridges.

7.4 Dual Elements: Dual elements in the balance may have their input and output wires paralleled inside the balance. These wire junctions are to be accessible without dismantling the balance.

8.0 CALIBRATION

8.1 The balance shall be completely assembled, aligned, and doweled before final calibration is done.

8.2 Full normal rated load shall be applied to each component in five or more equal increments in both positive and negative directions. The normal rated loads are specified in Section 6.2.1.

8.3 Forward normal force, aft normal force, forward side force, and aft side force will each be loaded in combination with axial force and rolling moment to their normal rated load, both positive and negative. The primary purpose of these combined loadings is to insure that there is no fouling inside the balance. Interactions of one component on another, as a result of combination loads, will have the same limitations as noted in Section 7.4.

8.4 The accuracy, repeatability, and hysteresis requirements, as specified in Section 7.0, shall be demonstrated prior to acceptance of the balance. Rockwell may, at its option, perform a full or partial acceptance calibration using Rockwell facilities. The supplier may witness this calibration.

8.5 The temperature stability shall be demonstrated by checking the bridge sensitivities at three stabilized temperatures between ambient and 460°F. The zero shift characteristics shall be demonstrated by recording the bridge outputs at five or more temperature settings between ambient and 460°F.

8.6 Balance proof loading shall be demonstrated by loading the balance to one and one-half times the normal rated load without changing the balance calibrations nor damaging the balance in any way. Loadings may be applied to each component separately.

8.0 CALIBRATION - Continued

8.7 All instrumentation used to calibrate the balance shall be in calibration by standards traceable to the National Bureau of Standards wherever NBS standards exist. In fields where there are no NBS standards good technical practice consistent with the state-of-the-art and requirements of the facility will be used to establish standards. The accuracy will not be rated better than the sum of the rated accuracy of the calibration standard and the maximum error obtained in calibration.

8.8 A complete calibration report shall be delivered within one week after delivery of the balance. The report shall contain photographs of all calibration setups.

9.0 EXTRA EQUIPMENT

9.1 Suitable calibration fixtures for loading and holding the balance during calibration shall be provided with the balance. The calibration body should have the capability of loading any or all components simultaneously, and in either direction.

9.2 The calibration body shall have loading points at the expected center of pressure of the model.

9.3 A master balance gage shall be provided with the balance. The master balance gage shall be constructed to within 0.0005" for linear dimensions, and from .0001" to .0003" larger for the outside diameter and to within .0001" for pin hole or key way dimensions. Angular dimensions shall be within 0.025° of arc.

9.4 Suitable carrying cases shall be supplied for all equipment supplied.

9.5 Leveling surfaces are to be provided on the calibration body.